

Single molecule diffusion in polymeric systems

by

Charmaine Sibanda

Thesis presented in fulfilment of the requirements for the degree of
Master of Science in Laser Physics in the Faculty of Science at
Stellenbosch University



Supervisor: Dr Gurthwin Bosman

Co-supervisor: Prof Erich Rohwer

April 2019

DECLARATION

By submitting this thesis electronically, I declare that the entirety of the work contained therein is my own, original work, that I am the sole author thereof (save to the extent explicitly otherwise stated), that reproduction and publication thereof by Stellenbosch University will not infringe any third party rights and that I have not previously in its entirety or in part submitted it for obtaining any qualification.

April 2019

Copyright © 2019 Stellenbosch University

All rights reserved

ACKNOWLEDGEMENTS

I thank the Lord God Almighty for granting this opportunity to me to undertake studies at Stellenbosch University and the strength to be able to complete this project.

I would like to express my deepest appreciation to my supervisors **Dr G. Bosman** and **Prof E. Rohwer** for encouraging me, teaching to work very hard and guiding me throughout the project. I would have never been able to complete this project without both their excellent guidance and patience as they helped me in improving my skills in experimental laser physics. I would like to thank **Prof E.G Rohwer** for allowing me to join the laser research institute (**LRI**), the great environment to undertake the project and for granting to me the **SARCHI** bursary to undertake studies with the physics department and thank **ALC Scholarship grant** for financial support. My sincere appreciation for the financial funding.

I thank my family and close friends for always believing in me and supporting me always.

Lastly but not least, I thank the LRI team at Stellenbosch University for their warm welcome to me and **Dina Ratsimandresy** for assistance with coding and image processing techniques.

DEDICATIONS

To my son, Melchizedek, may you always strive to attain you dreams and goals.

ABSTRACT

Single molecule diffusion in polymeric systems

Charmaine Sibanda

Department of Physics,

University of Stellenbosch,

Private Bag X1, Matieland 7602, South Africa.

Thesis: MSc

April 2019

The dynamics of thin polymeric systems were studied in this research work using the diffusion of single fluorescent molecules observed by single molecule fluorescence microscopy. A wide field single fluorescence microscopy setup was designed together with a custom-built heating stage to study the nano-environments of two different polymeric systems and how these systems are affected by a change in temperature. The designed optical setup achieved a localization precision of 20 nm which further enabled the tracking of single molecules embedded in polymeric systems. The position trajectories of the single molecules in the polymer matrices are used to calculate the motion of the single molecules from which the diffusion coefficient data is extracted. The distribution of the diffusion coefficients is a consequence of the microscopic dynamics of the polymeric systems coupled to the probe molecules. The fluorescence intensity pattern analysis of the single molecules is also used as reporters of the nano-environment of thin polymeric films.

UITTREKSEL

Die dinamika van dun polimeerstelsels is bestudeer in hierdie navorsingswerk met behulp van die diffusie van enkele fluoereserende molekules waargeneem deur enkelmolekule fluoressensie mikroskopie. 'n Wye veld enkel fluoressensie mikroskopie opstelling tesame met 'n toepaslike monster verwarmingstoestel is ontwerp om die nano-omgewings van twee verskillende polimeerstelsels te bestudeer onder die geringste temperatuurverandering. Die optiese opstelling het 'n enkelmolekuul lokaliserings-presisie van 20 nm behaal. Hierdie aansienlike presisie het toegelaat dat die posisies van die enkele molekules in die polimeermatrikse gebruik word om die diffusie-koëffisient van die enkele molekules te bereken. Die verspreiding van die diffusie koëffisiënte is 'n gevolg van die mikroskopiese dinamika van die polimeerstelsels gekoppel aan die molekules. Die enkelmolekuul fluoressensie intensiteit word ook ontleed en daar word getoon dat daar 'n definitiewe monster afhanklikeheid bestaan.

Table of contents

DECLARATION	ii
ACKNOWLEDGEMENTS	iii
DEDICATIONS	iv
ABSTRACT	v
UITTREKSEL	vi
Table of contents	vii
Table of figures	ix
Chapter 1: Introduction	1
Chapter 2: Literature review	2
2.1 Polymers	3
2.2 Effect of temperature in polymers	5
2.3 Model/s for glass transition theories.....	8
2.4 Fluorescence imaging	11
2.5 Single molecule fluorescence microscopy- An application to polymer research	14
Chapter 3: Experimental procedures.....	16
3.1 Fluorescence microscope imaging setup	17
3.2 Sample preparation	19
3.3 Setup characteristics	22
Chapter 4: Results and discussions	28
4.1 Polymer relaxation processes below T_g	29
4.2 Static heterogeneity for PBI in Ps film below T_g	32

4.3 Single molecule diffusion of PBI in Pibma below T_g	37
Chapter 5: Conclusions	46
BIBLIOGRAPHY	48

Table of figures

- Figure 1. Formation of polystyrene through vinyl polymerization, which is an example of addition polymerization. the carbon double bond is broken by the free radical and a polystyrene polymer is formed. Image taken from [7]. _____ 3
- Figure 2. Condensation polymerization of a carboxylic and amine monomer to produce a polyamide Nylon. _____ 4
- Figure 3. Difference in physical chain segment structure of polymers. Amorphous polymer chain segments are disarranged, and semi-crystalline polymer chain segments have some degree of order within the polymer chain, image adapted from [8]. _____ 4
- Figure 4. Effect of temperature on amorphous and semi-crystalline polymer chain segments. At low temperatures both chain segments are brittle and immobile, as temperature is increased, a region where polymer segments are rubbery, and mobile is reached called the glass transition temperature. This temperature region affects the processing and application of polymers. Semi-crystalline polymers have a melting temperature due to the ordered nature of the chain structure and as a result have a narrow processing range. Amorphous polymers have no definite melting temperature a direct consequence of the disarranged chain structure and thus have a broad processing range. Image adapted from [10]. _____ 6
- Figure 5. Typical schematic showing non-Arrhenius α -relaxation process and Arrhenius β -relaxation process as function of inverse temperature. Deviation from the Arrhenius behavior of the alpha process is due to the heterogeneities arising from the motion of the main chain long-range motion that is frozen in the glassy state to result in slow dynamics. _____ 8
- Figure 6. A graph plotted from simulated results using equation (v), with $T_g = 56$ °C. As the temperature is decreased towards the glass transition temperature, the viscosity of the polymer is expected to increase. However, as the glass transition is approached (< 65 °C), viscosity increases by orders of magnitude due to heterogeneities associated with α -relaxation processes and for temperatures at and below the glass transition temperature, the free volume theory fails to explain effects of heterogeneous dynamics. _____ 10
- Figure 7. A Jablonski diagram is used to describe fluorescence emission. The molecule absorbs energy from ground state S_0 and is excited to first excited state S_1 , the excited molecule collides with surrounding molecules and loses energy

non-radiatively before falling to S_0 emitting a photon in the form of fluorescence. The molecule can undergo nonradiative transitions through intersystem crossing (ISC) due to singlet-triplet spin-orbit coupling. From the lowest excited triplet state the molecule can either return to singlet ground state through phosphorescence or undergo a permanent change due to photo dynamics interactions rendering its ability to fluoresce thereby becoming going into a photobleached state. _____ 12

Figure 8. A typical wide field fluorescence microscopy set up, the sample area imaged is large and excitation is from a collimated laser beam that is focused on the back-focal plane of the objective. The fluorescence emission from the sample is collected through the same objective and is separated from the incident excitation laser beam using a dichroic mirror and suitable filters and finally detected using a scientific CCD camera Image taken from [14]. _____ 13

Figure 9. (a) Experimental setup that was used for imaging single molecules embedded in a thin polymer film sample. ND- neutral density filters, RM- reflecting mirror, WP- quarter waveplate. AL - aspherical lens, SMF - single mode fiber, PL - pre-focusing lens, DBS- dichroic beam splitter, Obj- microscope objective, NF- notch filter, FM- flip mirror, AD- achromatic doublet, BF- bandpass filter. (b) Graph showing how stable the incident light was after coupling it through a single mode fiber, coupling efficiency was calculated to be 40 %. _ 17

Figure 10. (a) Experimental set-up to produce circularly polarized light through the insertion of a quarter waveplate. A linear polarizer was also introduced and was rotated in front of a power meter used to check the intensity of the polarized light. ND- neutral density filters, RM- reflecting mirror, WP- quarter waveplate, AL- aspherical lens, SMF- single mode fiber, CL- collimating lens, LP- linear polarizer, PM- power meter. (b) Graph shows the power intensity stability measured as the linear polarizer was rotated. From the graph it can be observed that the power intensity remained constant as the angle of rotation, thus the indicating that the polarization state of the excitation light was successfully changed to circular. _____ 19

Figure 11. The thickness of polystyrene films is determined using the ratio of absorbance of liquid polystyrene solution (a) and that of a solid polystyrene film spin-coated on a MgF slide (b), were the absorbance is proportional to the density of the material and its length/thickness. The absorbance of the liquid polystyrene liquid solution was measured to be 0.5 and that of the polystyrene film 0.1. _ 22

Figure 12. Image on the left shows the grayscale image of the calibration grid and on the right, the intensity profile resulting from cutting along a horizontal line drawn across the grid using ImageJ. 270 pixels counted on camera represents $10\mu\text{m}$ in real space dimensions of the grid imaged. _____ 23

Figure 13. Localization precision of single fluorescent perylene dye molecules embedded in polystyrene (circled in red) were imaged over 100 frames, camera exposure time of 500 ms and at a temperature of $17\text{ }^\circ\text{C}$. The loci of the individual emitters were used to calculate the localization precision in both the $X\ \sigma = 5\text{ nm}$ (bottom left) and $Y\ \sigma = 6\text{ nm}$ (bottom right) directions. The deviation in the localization precision is a result of the polymer chain nano-environment which is known to be complex as was studied by Tomczak et al [34]. _____ 24

Figure 14. Image on the left shows three $2\ \mu\text{m}$ fluorescent microspheres acquired over 30 mins and used to characterize the microscope stage drift dynamics. The stage drift dynamics are characterized using the diffusion coefficient of the microspheres extracted from the slope of the MSD graph (right). _____ 25

Figure 15. Heating setup used for heating polymer samples. The mechanisms employed to heat the samples is Joule heating, where a current is passed through the resistive ITO cover slide which then heats up as the charge carriers interact, collide and scatter from the ITO atomic ions, thereby producing thermal energy. _____ 27

Figure 16. The graph shows that the heat energy is directly proportional to the voltage, current and thus an increase in voltage and current results in an increase in thermal heat energy. _____ 27

Figure 17.a) The structure of the PBI dye molecule that was embedded in two different polymer environments. The polymers that were used in this research work are Pibma with glass transition temperature of $55\text{ }^\circ\text{C}$ (b) and Ps with a lower glass transition temperature of $100\text{ }^\circ\text{C}$ (c). _____ 29

Figure 18. Image sequences of PBI dye molecules embedded in a Pibma (a) and Ps (b) film at an exposure time of 200 ms and $18.5\text{ }^\circ\text{C}$. A notable difference between the two polymers on the fluorescence emission of PBI is the number of observable single molecules and the photobleaching of PBI molecules in Ps film. _____ 30

Figure 19. (a) Insert show the typical blinking behavior of single molecules in the thin polymer films. (b) Influence of polymer environment to single fluorescent molecules emission. From the Ps film, the individual fluorescent probes were noted to photo blink and most photo bleaching as a function of time. The Pibma

film showed the number of fluorescent probes to relatively stay the same across each image frame and photo blinking was observed. _____ 31

Figure 20. Narrow distributions of the diffusion coefficients of PBI in Pibma (on the left-hand side) and Ps (on the right-hand side) thin films imaged at 18.5 °C show that far below the glass transition temperature the polymer chains and segments are rigid. The rigidity of the polymer chains and segments means reduced free volume distributions in the polymer or the caging effects that hinders motion of small probe molecules within the polymer film at very low temperatures below T_g [37]. _____ 32

Figure 21. Static heterogeneities of polystyrene were studied by observing the photo physical changes of PBI in air as a function of temperature. Photo blinking and photo bleaching of single molecules was observed with increased photo bleaching for PBI in air. _____ 33

Figure 22. Static heterogeneities of polystyrene were studied by observing the photo physical changes of PBI in a Ps film as a function of temperature. The number of observed single PBI molecules in a Ps film increase as compared to single PBI molecules on a plain ITO cover slide. _____ 34

Figure 23. The effective photo bleaching rate reduces as temperature is increased for PBI in Ps film 23 ms to 18 ms for 18.5 °C and 43.5 °C respectively (on the left-hand side). The effective photo bleaching rate PBI in air is approximately constant ~8 ms for both temperatures (on the right-hand side). The effective photo bleaching rate was extracted from the slope of the linear fit graph. _____ 35

Figure 24. The average intensity count for PBI in Ps film was lower than that of PBI in air (top graph). Fluctuations in the average intensity trace of PBI as the temperature is increased (left) is attributed to the static heterogeneities within the polymer film that include different amounts of free volume distribution, enhanced surface interfaces because of the thin film and local density fluctuations of the polymer chain segment structure. The excited PBI probe molecule fluorescence emission was influenced by the interactions between the polymer film and the amount of oxygen that could diffuse through the polymeric film as the temperature is increased these interactions also increased and contributed to the photo bleaching of PBI dye molecules in the Ps film (right). 36

Figure 25. a) Zoomed in image of individual fluorescent molecule, the red pattern is the trajectory length indicating movement of the molecule. b) the loci position shifts from the initial start coordinate illustrate how the molecule moved in the x

and y directions, movement is isotropic from the histogram distribution and can be assumed to be Brownian. _____ 38

Figure 26. By tracking the molecule movement in the polymer, the mean square displacement is extracted at each time lag of 200 ms and from which the slope of the MSD plot gives the diffusion coefficient of an individual PBI in Pibma film.

_____ 39

Figure 27. Diffusion coefficients of PBI in Pibma at four different temperature ranges indicates that as the temperature is increased the standard deviation of the diffusion coefficients increases due to the heterogeneous cooperatively rearranging regions. As the T_g for Pibma is slowly approached the translational diffusion of the PBI reduced. _____ 40

Figure 28. The Vogel-Fulcher law fails to describe the viscosity temperature dependence of the diffusion coefficients of PBI molecules in Pibma due to heterogeneities in the thin film as shown in the plot of $\ln(D)$ against temperature (left). A plot of the standard deviation of the diffusion coefficients illustrates the increase of heterogeneities as the temperature is increased until the approach of T_g of Pibma (55 °C), where the translational diffusion processes are slowed down (right). _____ 41

Figure 29. Cooperatively rearranging regions within a polymer have been said to cause a caging effect on probe molecules embedded in the polymer film. At low temperatures below the T_g of a polymer film, each size of the CRRs is large and the number of the polymer segments large and motion of the regions is through vibrations which are coupled to the probe molecules and the relaxation process associated with this motion is the β -relaxation. As the temperature is increased towards T_g , the size CRRs reduces and the number of polymer segments within the CRRs reduces hence breaking the caging effect on the tracer molecules [25], [34], [50]. The cage breaking effect enhances the diffusion of the probe molecules within the polymer film and the relaxation process associated with this motion is the α -relaxation process. _____ 42

Figure 30. Enhanced surface interfacial interactions cause heterogeneities that contribute to T_g shifts in thin polymer samples as compared to their bulk counterparts [53], [54]. The reduced polymer chain density at the surface assists the diffusion motion of individual fluorescent tracers across the film, however the local density distribution of amorphous polymer chains is random thus the motion of the probe molecules is also expected to be inhomogeneous. _____ 43

Figure 31. Decreasing average fluorescence intensity of PBI single molecules in Pibma as temperature was increased was observed. _____ 44

Chapter 1: Introduction

Thin polymeric systems have become very important materials due to their unique adjustable physical properties. This is evident through reports that indicated the rise in polymer production which was pegged at 8.3 billion tonnes in 2017 [1]. The physical properties of thin films are important for different industrial sectors such as the coating and adhesives sector, biomaterials sector amongst many others. Temperature is known to affect the physical properties of thin polymeric systems which are a consequence of microscopic dynamics of the polymers and affect the application of the polymer through its service temperature. One such unique property of thin polymeric systems is the reduction of their service temperature in comparison to a thick film of the same material. Bulk polymer research studies have been vastly conducted many decades before, however thin polymeric system dynamics, in particular the glass transition shifts are still not yet fully understood [2]. Hence further need arises to employ experimental and theoretical tools in understanding thin polymeric film systems.

The technique that was employed in this work to study the dynamics of thin polymeric systems was single molecule fluorescence microscopy. Advantages of using this technique include direct observation of single molecules thereby eliminating the need for ensemble averaging which obscures complex properties in bulk measurements [3] and the sensitivity of fluorescence to minute changes in the probe environment means that fluorescent probes become a natural choice as a molecular reporter of thin polymeric system. By tracking the single molecule position through diffusion processes and analyzing its fluorescence intensity in a polymeric system enables us to study the microscopic dynamics of the polymeric systems.

The work in this research project covers discussions on definitions of polymers and how they are made and the effect of temperature and glass transition temperature of polymeric systems. Further information is given in Chapter 2 on bulk polymer models and how these models have been used in trying to explain heterogeneities in polymers and application of single molecule fluorescence microscopy to polymer research is introduced in the same chapter. The design of the optical setup that was used and its characterization is given in Chapter 3 that enabled the study of diffusion of single molecules in polymeric systems. The results and discussions of the measurements of single molecule motions and fluorescence emission trajectories observed when the dye molecules were embedded in different polymeric systems are analyzed and the causes of diffusion processes related to microscopic dynamics of the polymeric systems are covered in Chapter 4.

Chapter 2: Literature review

Polymers are materials composed of high relative molecular mass built from repeat units of low relative molecular mass. World production of polymers has been pegged at over 8.3 billion tonnes in 2017 which in turn has also increased the necessity for sustainable options for polymer production, recycling and waste management [1]. The high demand of polymers has made them become one of the most important in the biomedical sectors related to biocompatibility of medical implants, drug delivery system and industrial sector related to protective and functional coatings [4]. The photophysics and photochemistry in polymer research has been central areas of interest in understanding the structure and dynamics of polymers. These materials have shown interesting and unique physical properties that change drastically such as viscosity and thermal expansion below, near and above the glass transition temperature which originate from complicated relaxation processes of polymer chains [5].

However, these unique properties have not yet been fully understood despite theoretical and experimental studies over the past decades. Hence the need to further study the temperature dependence of the physical properties of polymers as they are of high crucial importance for various applications. Different experimental methods have been used to try understanding the nano-environment of polymers. One of these methods also used in this research and described in greater detail in this chapter, is single molecule fluorescence microscopy. It is a powerful imaging technique that enables the direct observation of single fluorescent molecules in their nano-environment. In this chapter more, detail is given on the definition of a polymer and how they are formed, then focus on temperature dependence of polymers, the consequence of these dependences to polymer chains and define what the glass transition temperature is. Also covered in this section is the models from past literature that have been used to try understanding the polymer nano-environment in different temperature ranges and finally why the use of single molecule fluorescence microscopy was chosen as a preferential technique about polymer dynamics.

2.1 Polymers

Polymers are macromolecules formed through polymerization and are composed of a basic repeat unit called a monomer [6].

The two main types of polymerization are addition/chain polymerization and condensation/step reaction polymerization.

Addition/Chain reaction polymerization

Addition polymerization is a three-step process. The process begins with initiation, then propagation and ends with termination.

Initiation- a double bonded carbon monomer reacts with a catalyst usually a free radical species. The double bond is broken and the monomer bonds to the free radical species an example is the formation of polystyrene where the styrene monomer reacts with a free radical to form polystyrene (Figure 1).

Propagation- in this step the styrene monomer units are added sequentially to the reactive chain molecule. The reactive site is transferred to each styrene monomer as it is linked to the chain which gets longer and longer.

Termination- this takes place when another free radical meets the ends of the long growing polymer chain. The free radical terminates the chain by linking with the reactive propagating polymer chain thus producing a complete polymer chain.

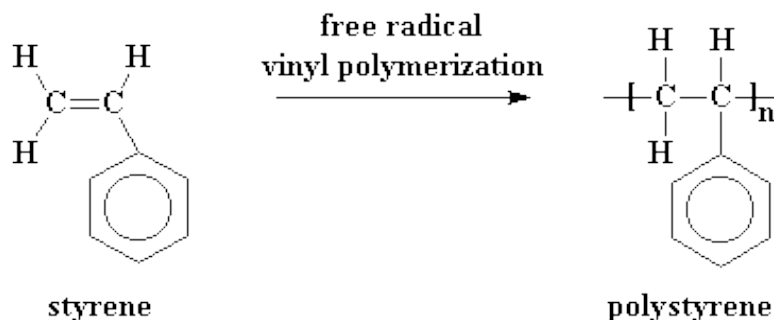


Figure 1. Formation of polystyrene through vinyl polymerization, which is an example of addition polymerization. the carbon double bond is broken by the free radical and a polystyrene polymer is formed. Image taken from [7].

Condensation polymerization

Condensation polymerization involves two different types of monomers that react through stepwise intermolecular chemical reactions to form a polymer chain, also a by-product is formed usually water

or methanol. In the example given below, a carboxylic acid monomer and an amine monomer join in an amide linkage to form a polyamide Nylon and a water molecule is removed (Figure 2).

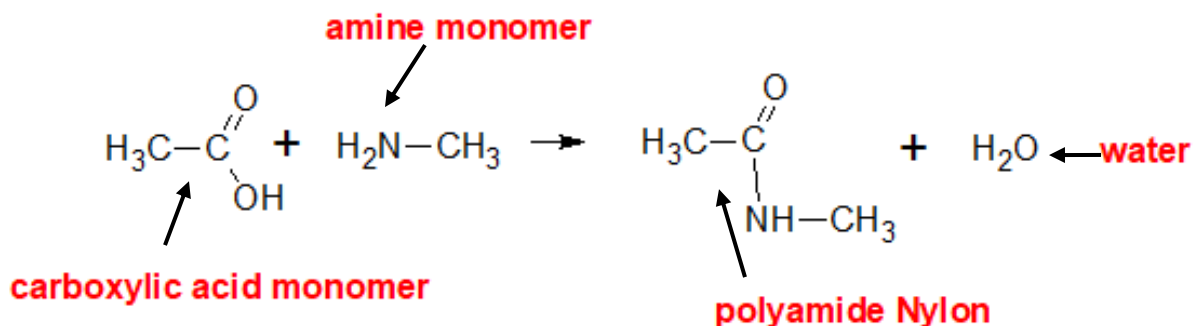


Figure 2. Condensation polymerization of a carboxylic and amine monomer to produce a polyamide Nylon.

2.1.1 Polymer physical structure

Polymer chain segments can exist in two distinct physical structures. These segments are either semi-crystalline or amorphous in form.

Amorphous polymers have a disarranged chain structure and semi-crystalline polymers have some degree of ordered arrangement of the chain segments. The difference in molecular segments between an amorphous chain structure which is entangled and randomly arranged compared to a semi-crystalline chain structure which shows some ordered arrangement of the chain segments (Figure 3).

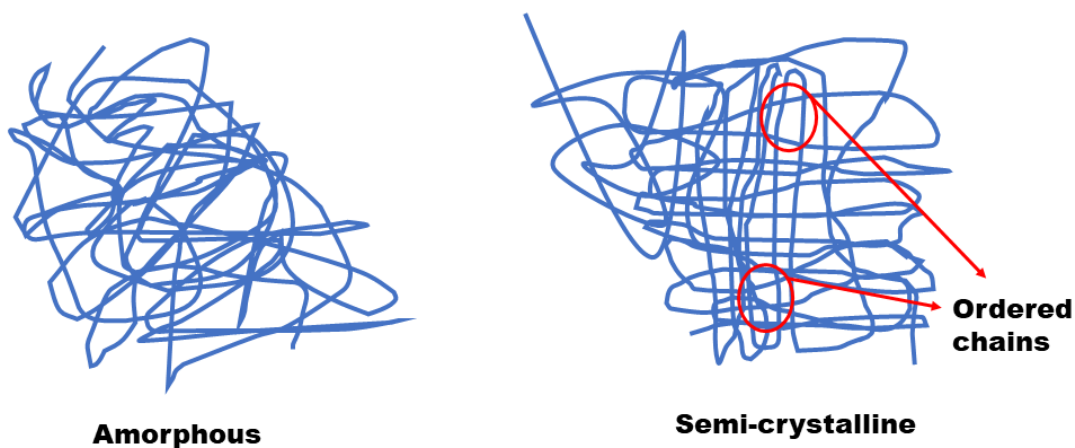


Figure 3. Difference in physical chain segment structure of polymers. Amorphous polymer chain segments are disarranged, and semi-crystalline polymer chain segments have some degree of order within the polymer chain, image adapted from [8].

2.2 Effect of temperature in polymers

The disarranged order of chain segments in amorphous polymers prevents them from having a definite melting temperature, in contrast the partially ordered arrangements of semi-crystalline chain segments gives this type of polymers a melting temperature.

At lower temperatures, the chain segments of polymers are often brittle and immobile, as the temperature is increased the molecular chain mobility is increased and at even higher temperatures the polymer chains flow as highly viscous liquids and form a visco-elastic material.

2.2.1 Glass Transition Temperature (T_g)

This is the temperature region where immobile polymer chain segments slowly soften to a rubbery disordered glassy state and a viscosity of 10^{12} Pascal-seconds (Pa.s) is reached, as the temperature is increased [9]. The glass transition can also be defined as the temperature where the average molecular relaxation time of the polymer sample material is approximately 100 seconds depending on the heating and cooling rates. The contrast in molecular chain motion between amorphous and semi-crystalline polymers as a function of temperature, below the glass transition temperature both chain segments are immobile, an increase in temperature sees an increase in chain mobility and flexibility, where the polymer undergoes a glass-rubber transition known as the glass transition temperature. This region is also known as the service region of polymers and directly influences the processing and application of polymers [10]. Using calorimetry experimental methods to investigate the response of polymers to heat results in a plot of heat flow against temperature. An increase in temperature from the heat flow versus temperature plot indicates a dip due to change in heat capacity that is reached after the plateau for semi-crystalline polymer chain segments, this dip marks the melting temperature for this polymer. For amorphous polymers, the chain segments flow as a visco-elastic material and show no definite melting temperature (Figure 4).

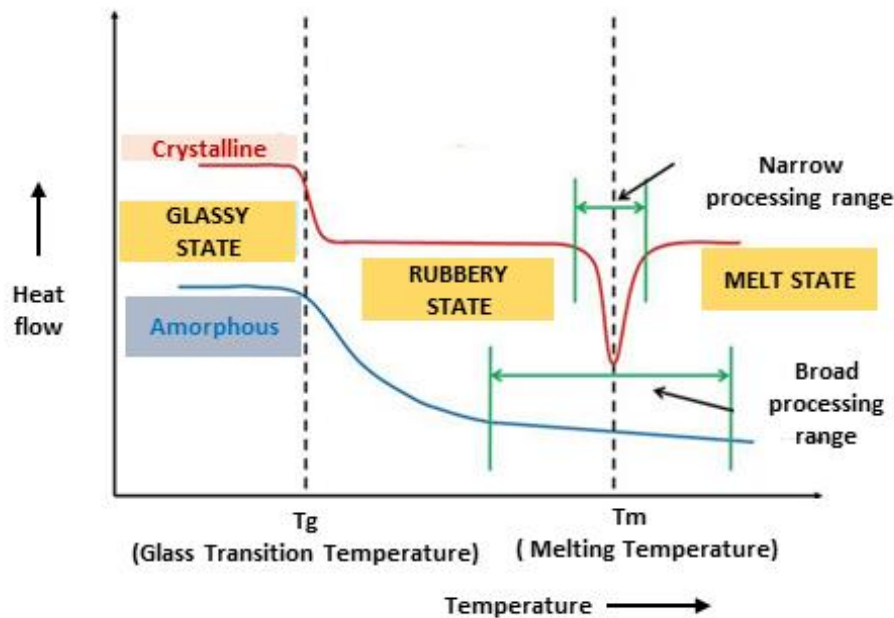


Figure 4. Effect of temperature on amorphous and semi-crystalline polymer chain segments. At low temperatures both chain segments are brittle and immobile, as temperature is increased, a region where polymer segments are rubbery, and mobile is reached called the glass transition temperature. This temperature region affects the processing and application of polymers. Semi-crystalline polymers have a melting temperature due to the ordered nature of the chain structure and as a result have a narrow processing range. Amorphous polymers have no definite melting temperature a direct consequence of the disarranged chain structure and thus have a broad processing range. Image adapted from [10].

2.2.2 Thin polymer film dynamics below and above glass transition

The physical properties of thin films are important for different applications such as coatings, adhesives, biomaterials amongst many others [11]–[13]. To be able to design a specific surface, there is need to be able to control film thickness, which in turn reveals different degrees of molecular motion for different thicknesses [14]. Thin polymer films have shown different properties at their interfaces as compared to thick films. One major difference is the reduction of T_g at the surface for thin films as compared to thick films, that is bulk T_g for the same polymer material. This decrease in T_g in thin films is attributed to enhanced surface mobility of the molecular chains due to a large surface to volume ratio of the nanometer scale films [15].

These associated changes in T_g due to enhanced surface mobility directly affect polymer dynamics. Different approaches have been used to directly study polymer dynamics such as the relaxation processes in polymers. At high temperatures, polymer chain segments have fast motions and very short relaxation time scales and at low temperatures, the molecular chain mobility decreases as the relaxation time scale

increases such that the chain segments are frozen before the system is in thermodynamic equilibrium [16]. The dynamics of amorphous polymers at temperatures below and near T_g are heterogeneous and above the T_g the dynamics are homogeneous. Heterogeneous dynamics show some regions of the polymer environment with high molecular mobilities whilst adjoining regions can exhibit slow molecular mobilities [17]. The two main relaxation processes that have been observed are alpha-relaxation and beta-relaxation processes [9]. The relaxation time refers to the time it takes for the polymer chains to respond to temperature changes.

Alpha relaxation- This is the primary relaxation process in most amorphous polymers and corresponds to structural relaxation or main chain long range motion of the entire polymer chain connected to viscous flow [18]. Alpha relaxation process shows a strong temperature dependence and exhibits strong spatial heterogeneities [9]. The temperature dependence of viscosity involving main chain long range motion, that is alpha relaxation, in a bulk polymer that has been cooled down from high temperatures show non-Arrhenius behavior known as the Vogel-Fulcher law [9]:

$$\eta(T) \propto \exp^{\frac{B}{T-T_{VFT}}} \quad (i)$$

B – is the activation energy equivalent parameter and T_{VFT} – Vogel Fulcher Tammann temperature which is the ideal glass transition temperature, typically 50 °C below the glass transition temperature, that marks the start of discontinuities in some thermodynamics quantities.

The Vogel-Fulcher law implies that at high temperatures above the glass transition, the viscosity of the polymer chain melt is low, and the polymer melt flows with less frictional resistance. As the polymer melt is cooled down, the viscosity of the chains gradually increases and at the glass transition temperature the viscosity increases by orders of magnitude and the polymer main chain motion become very slow compared with the experimental time scales, that is viscosity of 10^{12} Pa.s is reached and relaxation time scale of 100 s.

Beta relaxation – this is the secondary relaxation process which is caused by local motion of polymer segments, small scale backbone fluctuations from main chain rotations, vibrations associated with motion of polymer side groups rotating around bonds linked to main chains and it shows very short time scales and Arrhenius temperature dependence [19]. Arrhenius temperature dependence equation (ii) and an Arrhenius plot can be drawn by taking the natural logarithm of equation (ii), which yields the same form as that for the equation of a straight line, whose gradient gives the activation energy parameter and the intercept gives the pre-exponential factor. From the Arrhenius plot, the alpha process diverges as it approached the T_g because of the long-time scales from the main polymer chain with long range motions coupled with orders of magnitude of viscosity (Figure 5).

$$\tau \propto \exp^{\frac{E}{k_b T}} \quad (ii)$$

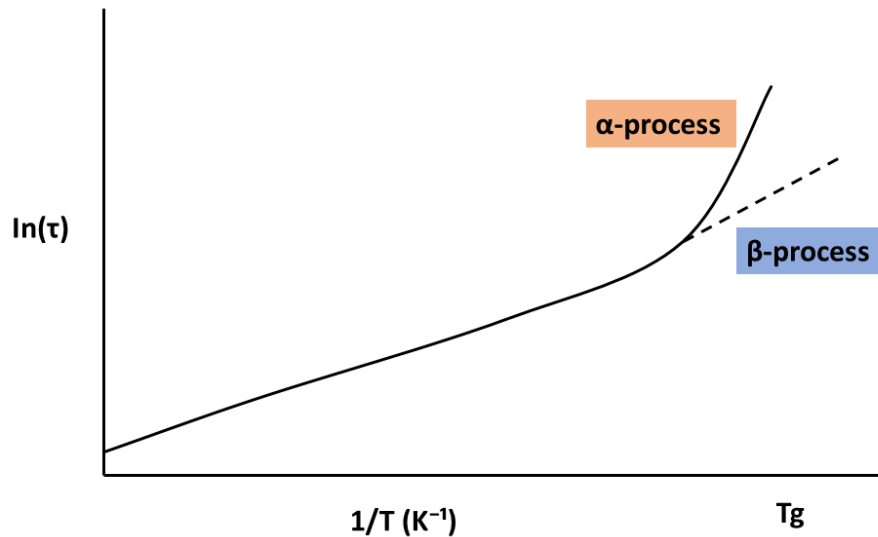


Figure 5. Typical schematic showing non-Arrhenius α -relaxation process and Arrhenius β -relaxation process as function of inverse temperature. Deviation from the Arrhenius behavior of the alpha process is due to the heterogeneities arising from the motion of the main chain long-range motion that is frozen in the glassy state to result in slow dynamics.

2.3 Model/s for glass transition theories

2.3.1 Free volume theory

In this theory the molecules in a polymer melt state occupy much of the melt's volume, partly as molecules that make up the monomers and partly as inaccessible volume that is blocked from access by steric factors. The remaining small fraction of volume is referred to as 'free' volume and is used for molecular motion [20].

For a polymer melt that is cooled from high temperature, the density is expected to increase as the free volume decreases, consequently the molecular motion is hindered, and the viscosity increases. According to Doolittle [21] the viscosity of a polymer liquid is related to the fractional free volume by equation (iii):

$$\eta \sim \exp \frac{bV_t}{V_f} \quad (\text{iii})$$

b - is an empirical unit-less constant. V_t and V_f is the total volume and fractional free volume respectively. At higher temperatures above the glass transition, the polymer chains occupy a large total volume, free volume increases also, and the viscosity reduces as the polymer melt flows easily. As the temperature is reduced, the free volume occupied by the polymer chains is reduced and the motion of the polymer chains is coupled to chain segments that move cooperatively and viscosity increases.

Doolittle made some assumptions to his equation that the activation energy for flow is inversely proportional to the fractional free volume V_f and the free volume has a linear temperature dependence above T_g given below:

$$V_f \propto (T - T_g) \quad (\text{iv})$$

The Doolittle equation can be combined with the assumption of linear temperature dependence of fractional free volume to get the modified Doolittle equation that relates the viscoelastic properties to the glass transition temperature.

$$\eta \propto \exp\left(\frac{b V_t}{(T - T_g)}\right) \quad (\text{v})$$

If the alpha relaxation process is being probed, then the viscosity is expected to increase by orders of magnitude as the glass transition temperature is approached as illustrated in Figure 6, showing simulated graph for equation (v) and polymer main chain motion is arrested. However, the free volume theory fails to explain dynamics observed below the T_g temperature for glassy polymers. The free volume values were extrapolated from differences in volume between a polymer that has been cooled below its T_g (that is in its glassy state) and a polymer melt cooled above its T_g (melt state) and large discrepancies between reported values for the value of free volume at glass transition have been reported ranging from 2.5-11.3% [22], thus indicating the need for further studies of amorphous polymer microstructure. The free volume theory is a statistical average quantity obtained from equilibrium states and moving towards glass transition from high temperatures, the state of the polymer is not in equilibrium state as a result using free volume theory in this temperature region obscures effects of heterogeneous dynamics. Studies have shown that there is no correlation between the free volume and the glass transition, that is, the glass transition of glassy polymers is not caused by the absence of free volume [23]. Therefore, a more direct knowledge of the microstructure of amorphous polymers is needed to verify the main assumptions made in the free volume theory and quantitative aspects of the free volume distribution and dynamics remain unknown.

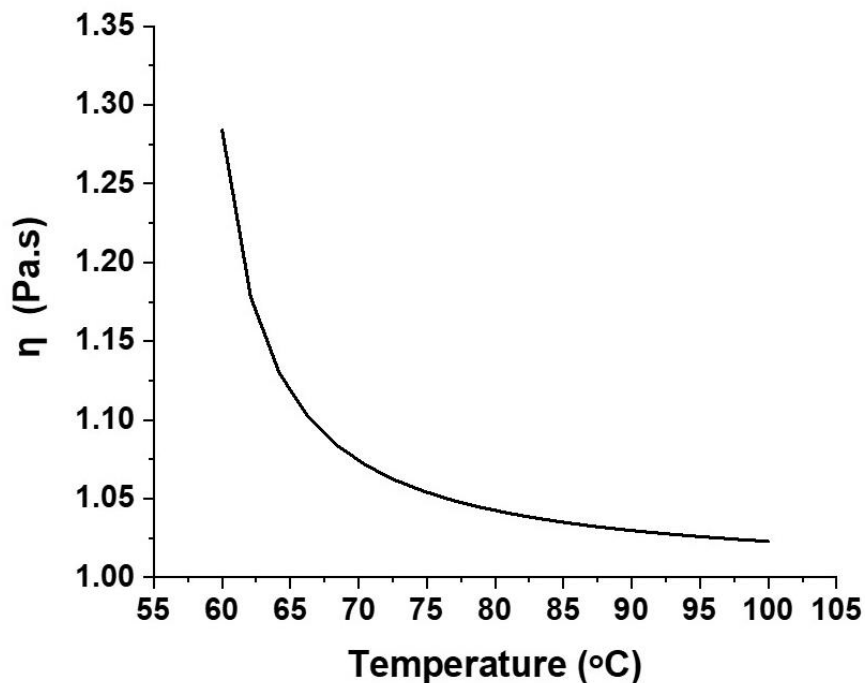


Figure 6. A graph plotted from simulated results using equation (v), with $T_g = 56$ °C. As the temperature is decreased towards the glass transition temperature, the viscosity of the polymer is expected to increase. However, as the glass transition is approached (< 65 °C), viscosity increases by orders of magnitude due to heterogeneities associated with α -relaxation processes and for temperatures at and below the glass transition temperature, the free volume theory fails to explain effects of heterogeneous dynamics.

2.3.2 Adam-Gibbs molecular-kinetic theory

The Adam-Gibbs theory describes the temperature dependence of relaxation time processes of polymers in terms of the disappearance of the configurational entropy of the cooperatively rearranging regions (CRR) [24]. The main assumption of this theory is that a polymer melt has several segments that cooperatively rearrange. The movement of the independent CRRs changes the configuration of the polymer system and this motion, determined via the diffusion constant given by equation (vi), is related to the configurational entropy S_c of the polymer system given by equation (vii) and temperature T [25].

$$D \propto \exp\left(\frac{-B}{T S_c}\right) \quad (\text{vi})$$

$$S_c = k_b \ln W_c \quad (\text{vii})$$

Here W_c is the number of configurations accessible by the system and k_b is the Boltzmann constant.

Each polymer chain segment is composed of monomers that rearrange themselves independently of its environment. At low temperatures the mobility of the polymer chain segment is very slow and individual chain molecular motion is absent, instead adjoining chain segments move by cooperative rearranging. As temperature is further reduced towards the glass transition temperature, the size of the cooperative rearranging regions CRR becomes larger and the configurational entropy of the system decreases, and this leads to an increase in viscosity. At even lower temperatures the configurational entropy becomes zero and the system exhibits one cooperatively relaxing region with no further freedom to rearrange its structure [26].

At the molecular level the dependence of the viscosity/relaxation time is given by equation (viii), where the viscosity and relaxation time depend on the number of chain segments which must move within the cooperatively rearranging regions.

$$\eta(T), \tau(T) = C \exp \frac{z^* \Delta \mu}{k_b T} \quad (\text{viii})$$

$\eta(T)$, $\tau(T)$ is the viscosity and structural relaxation time at a given temperature T respectively, C is a constant, z^* is the number of monomer units contained in the smallest region capable of rearranging, $\Delta \mu$ is the energy barrier for the chain segments to move, k_b is the Boltzmann constant.

Despite the success of the Adam-Gibbs theory of being able relate the microscopic dynamics of the CRRs to macroscopic configurational entropy of glassy polymers, it does not predict the size of the CRRs nor the explicit dependence of the CRRs to temperature.

2.4 Fluorescence imaging

This is the imaging of fluorescing molecules using a fluorescence microscope. A fluorophore¹ can either be in the singlet ground state or once radiated by electromagnetic radiation within the absorption spectrum of the fluorophore is excited to the first singlet state. Typically, the fluorescence of a molecule is described using a Jablonski diagram (Figure 7). The excitation of a fluorophore as it absorbs energy from the singlet ground state and reaches higher vibrational levels of the first excited singlet state. It then loses its excess of vibrational energy and relaxes to the lowest vibrational level of the excited state. The fluorophore continues to lose energy until the lowest vibrational level of the first excited state. From the lowest vibrational level of the first excited state, it can relax to any of the vibrational levels of the ground state and emits a photon in the process as fluorescence.

The excited molecule has a chance to undergo intersystem crossing to the excited triplet state due to spin-orbit coupling that causes the single molecule to flip its spin and end up on the triplet state. If the lowest triplet state remains occupied, the transition from the singlet ground state to the first excited singlet state does not occur and fluorescence emission is temporarily interrupted, and the molecule is said to be in a dark state. The molecule relaxes back to the singlet ground state from the triplet excited state through phosphorescence. After decaying from the triplet state to the singlet ground state, the molecule starts to

¹ Fluorophores are typically polyaromatic hydrocarbon molecules that re-emit light upon optical excitation [57].

fluoresce, and this phenomenon is called photo blinking and it is a reversible process. Fluorescence photons are emitted in bunches and separated by photo blinking periods, which occur when the molecule is in the triplet state. The triplet state lifetimes are dependent on the concentration of molecular oxygen. Fluorescence emitted by all fluorescent dyes fades during observation and this involves a photo chemical modification of the dye and results in irreversible ability of the dye molecule to fluoresce. A molecule in the excited triplet state can undergo a permanent change that renders its ability to fluoresce, thereby becoming a photo bleached molecule. The main cause of photo bleaching of fluorescent single molecules is due to photo dynamic interactions between the excited fluorophores and molecular oxygen in its triplet ground state.

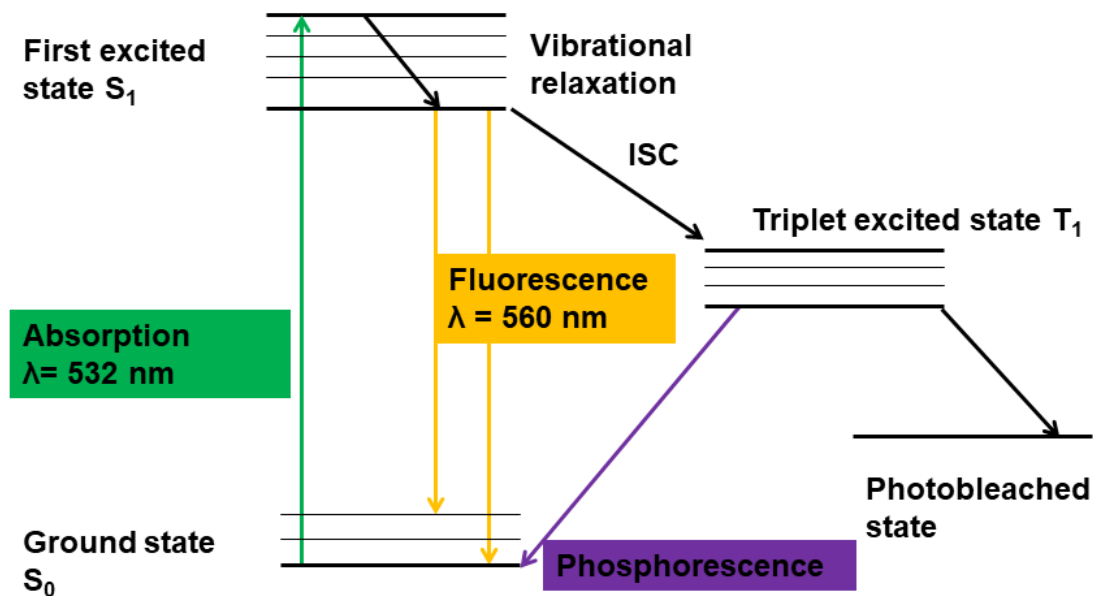


Figure 7. A Jablonski diagram is used to describe fluorescence emission. The molecule absorbs energy from ground state S_0 and is excited to first excited state S_1 , the excited molecule collides with surrounding molecules and loses energy non-radiatively before falling to S_0 emitting a photon in the form of fluorescence. The molecule can undergo nonradiative transitions through intersystem crossing (ISC) due to singlet-triplet spin-orbit coupling. From the lowest excited triplet state the molecule can either return to singlet ground state through phosphorescence or undergo a permanent change due to photo dynamics interactions rendering its ability to fluoresce thereby becoming going into a photobleached state.

Using spatially resolved imaging this fluorescence can be imaged using a microscope. One such microscope that is used to image fluorescence is wide field fluorescence microscopy. The microscope set up is designed in such a way that allows the separation of the intense optical excitation from the relatively weak fluorescence using appropriate dichroic mirrors [27]. A typical wide field fluorescence microscopy set up comprises a laser beam used as the exciting incident light, which is collimated and focused at the back-focal plane of high numerical aperture objective to achieve a uniform field of illumination for the sample (Figure 8). The emission is then collected via the same objective and passes through the tube lens and filters to separate the excitation light and imaged onto an imaging sensor (CCD – charged couple device or CMOS – complementary metal-oxide semiconductor).

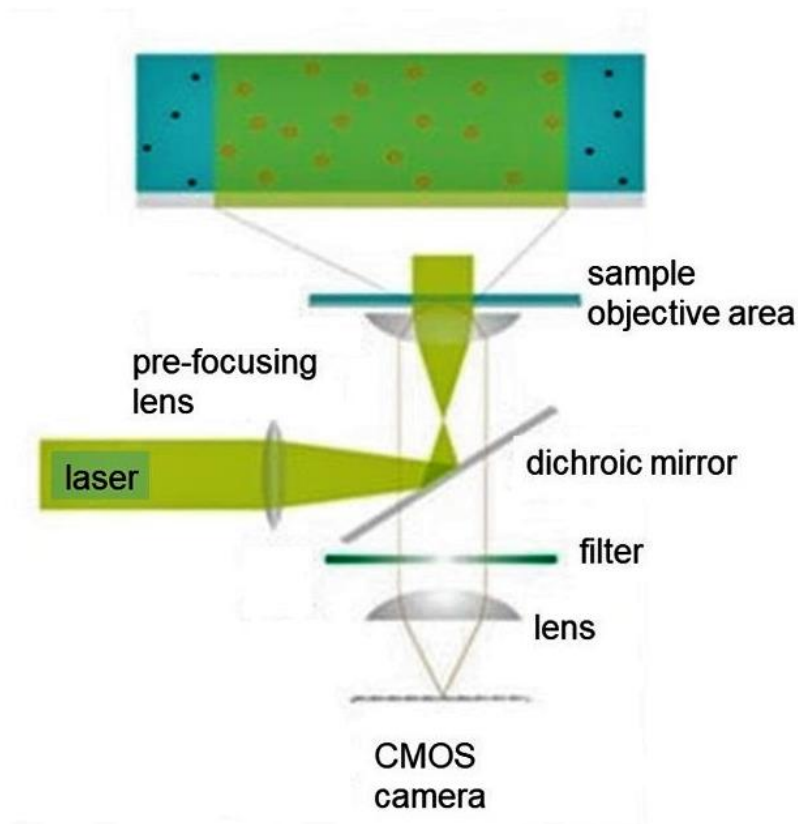


Figure 8. A typical wide field fluorescence microscopy set up, the sample area imaged is large and excitation is from a collimated laser beam that is focused on the back-focal plane of the objective. The fluorescence emission from the sample is collected through the same objective and is separated from the incident excitation laser beam using a dichroic mirror and suitable filters and finally detected using a scientific CCD camera Image taken from [14].

Some parameters that can be extracted from fluorescence microscopy are:

- i) Fluorescence intensity
- ii) Molecule position
- iii) Fluorescence lifetime

The advantages that have made fluorescence microscopy especially single molecule resolved fluorescence an invaluable imaging technique which allows the observation of smaller and smaller objects with great optical resolution that is below the diffraction limit include:

- i) High sensitivity of fluorescence to changes in fluorophore environment thus can be applied in different research fields such as studying polymer dynamics in their nano-environment.
- ii) Single molecule detection has enabled the ability to track and manipulate the individual emitters. This technique of being able to view one single emitter at a time eliminates the tendency of ensemble averaging.

- iii) Another advantage is that fluorescence lifetimes are very sensitive to the properties and changes of the probe molecule environment, as a result this means fluorescent probes become a natural choice as molecular level reporter of nano-environments.

2.5 Single molecule fluorescence microscopy- An application to polymer research

Different experimental methods have been used to try understanding the glass transition temperature and polymer nano-environment dynamics using dielectric spectroscopy to study segmental dynamics of polymers [28]. Pulse-gradient nuclear magnetic resonance has been used for self-diffusion and cooperative diffusion studies of polymer chains [29]. However most of the methods use ensemble averaging which obscures direct information on the heterogeneities in polymer diffusion, these heterogeneities are a direct consequence of microscopic dynamics in polymers and play a vital role in understanding numerous properties of polymers needed for processing and application industries.

As have been mentioned in the previous section, single molecule fluorescence microscopy is a powerful tool that enables the observation of single fluorescent molecules and the use of single fluorescent emitters to study and investigate the dynamics in polymer films below, near and above the glass transition temperature [30] and has shown heterogeneities in translation diffusion of single fluorescent probes as was illustrated by [9].

Far below the T_g temperature, the polymer segments are essentially frozen, however the polymer can still relax by local rearrangements of the chain segments. Any fluctuations of the polymer nano-environment can be observed by embedding dye molecules in the polymer matrix. These local density fluctuations affect the photophysical properties of single fluorescent molecules, such as photo blinking and photobleaching. It has been observed experimentally that the fluorescence lifetimes of the individual dye molecules in the polymer matrix is influenced by the local chain segment motion and distribution of the adjoining polymer segments by Vallee et al [5]. Because of the distribution of density of local polymer segments, changes of the radiative lifetimes of the individual fluorescent molecules reflect the dynamics of the polymer segments on a nanometer range such as the β relaxation process [5].

Near the T_g temperature, cooperative rearranging regions of the polymer matrix induce rotational orientation of the embedded dye molecules. The rotational motion of the individual dye molecules in the polymer matrix can be tracked by analyzing the polarization of the emitted fluorescence signal. Spatial heterogeneities near T_g showing exchange between fast and slow dynamics of rotational reorientation have been observed by Zhang et al [31].

For higher temperatures, that is $T > 1.2T_g$, translational diffusion of the single fluorescent molecules has been observed by Schob et al [32] which elucidates the dynamics and structure of the polymer nano-environment. If the α relaxation process is being probed and the viscosity is inversely proportional to the diffusion coefficient according to the Einstein-Stokes law, then the diffusivity motion of single molecules embedded in a polymer matrix is expected to follow the Vogel-Fulcher relation equation (ix) that resembles the bulk polymer viscosity temperature dependence equation (v):

$$D = \exp^{\frac{-B}{R_0(T-T_{VF})}} \quad (\text{ix})$$

Here B is an activation energy parameter, R_0 is the ideal gas constant and T_{VF} is the Vogel temperature which describes the ideal glass transition temperature.

For this project, thin polymer film dynamics were investigated using single molecules as the nano-environment probe far below T_g , towards and near T_g of the polymer film. The experimental procedure and sample preparation are covered in Chapter 3.

Chapter 3: Experimental procedures

Single molecule fluorescence microscopy is an invaluable imaging tool as it enables the direct observation of single fluorescent emitters and obscures ensemble averaging. Thin polymer film dynamics were investigated using single fluorescent molecules as the nano-environment probe. The high sensitivity of fluorescence to minute changes in the polymer nano-environment permits the detection and tracking of the fluorescent emitter and from the data extracted linked to dynamics of the polymer nano-environment. The data is used to further understand the dynamics of thin polymer films and dependence to temperature variations which influences their applications. Thin polymer films were made through a spin coating procedure, the thickness of the films was determined using UV-Vis spectroscopy. Sample preparation protocols for thin polymer films and embedding single molecule emitters in thin polymer films is given in greater detail in this chapter. Fluorescence signatures from perylene dye embedded in two different polymers were studied using wide-field fluorescence microscopy.

The set-up comprises of two main elements, the first element consists of the optical illumination path where a 532 nm solid state laser was coupled to the microscope through a single mode optical fiber and used to excite the dye molecules spin coated onto a glass cover slide. As the single molecules relax back to their ground state, they fluoresce, and the fluorescence emission was imaged via the second element, the optical imaging path, comprising of a collection of lenses and optical filters and a CMOS camera. Both the optical illumination and imaging paths consist of other optical elements that made it possible to image the fluorescence signatures of the dye molecules embedded in thin polymer films and is discussed further in more detail in the following subsections. The imaging characteristics of the system discussed are the image calibration, localization precision and system drift analysis using microparticles. The heating set-up for the investigation of influence of temperature on the dynamics of thin polymer films is also explained and analyzed in this chapter.

3.1 Fluorescence microscope imaging setup

The illumination source is a diode pumped solid state Nd: YAG continuous wave laser emission centered at a wavelength of 532 nm with an output power of 520 mW (LCX: Oxxius - 532). To obtain uniform illumination the laser is coupled into a single mode fiber (SM450, Thorlabs) using an aspherical B-coated lens. The other end of the fiber was coupled into the inverted microscope using a fiber coupler and a collection of lenses, to ensure that the laser beam was focused on to the back focal plane of an oil objective. The coupling efficiency of the system was also calculated (Figure 9b).

The fluorescence emission from the samples were collected using by a Nikon objective (Plan Fluor 100x/1.30 oil) and separated from the laser light using a dichroic mirror. The dichroic mirror working principle is based on constructive and destructive interference as it has multiple dielectric coatings, which reflects and transmits light of a certain wavelengths differently, for this setup the dichroic mirror (FF535-SDi01, Semrock) transmitted light below 532 nm and reflected light above 532 nm. The excitation light is further suppressed by a notch filter that rejects the 533 nm wavelength for transmission ($533 \text{ nm} \pm 10 \text{ nm}$, Thorlabs) and further focused using an achromatic doublet, which was used to limit the effects of spherical aberrations and constituent color separation of the transmitted light (AC508-200-A-ML-400-700 nm, Thorlabs). A bandpass filter was used to transmit the sample emission light of wavelengths of $565 \text{ nm} \pm 24 \text{ nm}$ (MF565-24, Thorlabs) and the transmitted light was then focused again using another achromatic doublet lens. The image is and finally detected using a CMOS camera (ORCA-Flash4.0 V2 C11440-22CU, Hamamatsu).

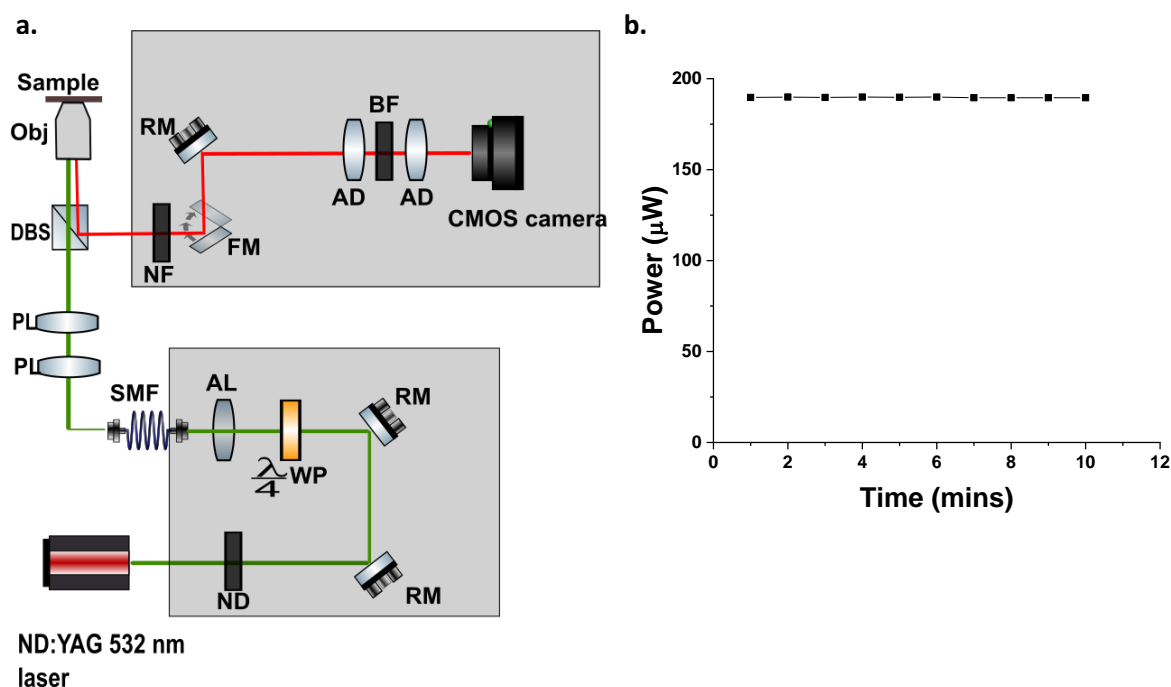


Figure 9. (a) Experimental setup that was used for imaging single molecules embedded in a thin polymer film sample. ND- neutral density filters, RM- reflecting mirror, WP- quarter waveplate. AL - aspherical lens, SMF - single mode fiber, PL - pre-focusing lens, DBS- dichroic beam splitter, Obj- microscope objective, NF- notch filter, FM- flip mirror, AD- achromatic doublet, BF- bandpass filter. (b) Graph showing how stable the incident light was after coupling it through a single mode fiber, coupling efficiency was calculated to be 40 %.

Changing polarization state of incident light

The polarization state of the incident laser light is linear, however to ensure that the single molecules (assumed to be electric dipoles which are randomly orientated) were excited uniformly the polarization state of the incident light had to be changed. Since the electric dipole moments of the single molecules are randomly orientated on the cover slide after spin coating and excitation using linearly polarized light will not ensure uniform fluorescence emission from all the single molecules. Therefore, the use of circularly polarized light ensures that the electric field of light is always appropriately orientated with respect to the transition dipole moment in the single molecules which has the desired effect of uniform excitation of all dipoles and subsequently the uniform emission of the fluorescence.

To achieve the aforementioned, the linearly polarized light was passed through a quarter waveplate positioned at 45° to its polarization axis to convert it to circularly polarized light. A quarter waveplate is made of birefringent material, that is a material with variations for index of refraction, because of these variations in the refractive index the orientation of the transmitted light is different and the phase between the two perpendicular polarization components of the transmitted light is shifted. To check if the linearly polarized light had changed to circularly polarized light, a linear polarizer was placed at one end of the fiber and a power meter also placed in front of the linear polarizer to measure the power intensity of the incident light as the linear polarizer was rotated. If the quarter waveplate was placed at an angle that ensures that linearly polarized light is changed to circularly polarized light, then the power intensity measured as the linear polarizer is rotated should remain constant since circularly polarized light has the same intensity in all directions (Figure 10).

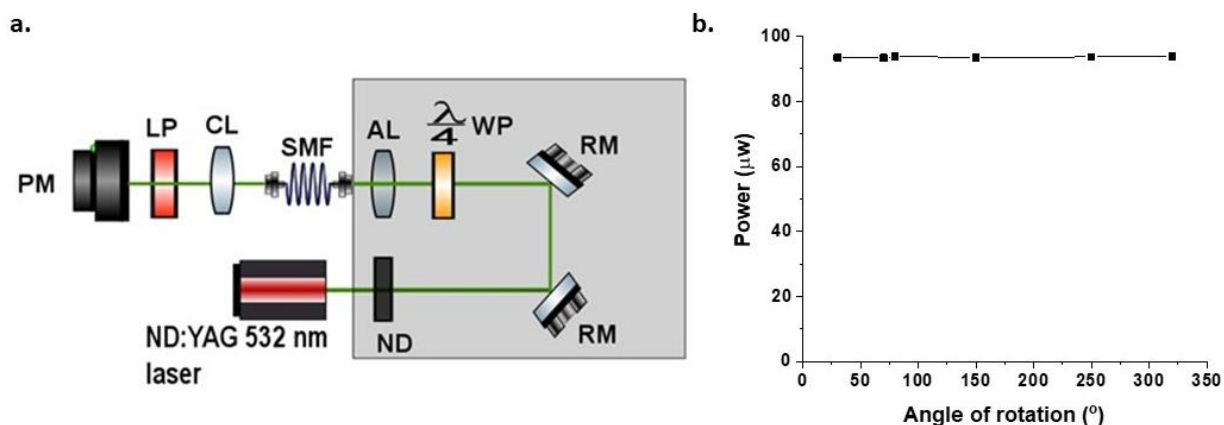


Figure 10. (a) Experimental set-up to produce circularly polarized light through the insertion of a quarter waveplate. A linear polarizer was also introduced and was rotated in front of a power meter used to check the intensity of the polarized light. ND- neutral density filters, RM- reflecting mirror, WP- quarter waveplate, AL- aspherical lens, SMF- single mode fiber, CL- collimating lens, LP- linear polarizer, PM- power meter. (b) Graph shows the power intensity stability measured as the linear polarizer was rotated. From the graph it can be observed that the power intensity remained constant as the angle of rotation, thus indicating that the polarization state of the excitation light was successfully changed to circular.

3.2 Sample preparation

In this section the preparation of single fluorescent molecules embedded in thin polymer films and deposited on glass cover slides will be discussed. Cleaning the glass cover slides also enhances the accuracy in the detection of the single molecules' fluorescence, hence it is crucial that the cover slides are thoroughly and properly cleaned.

3.2.1 Cover slide cleaning

The glass slides are cleaned to remove any particulates that might fluoresce and affect the results.

The cover slides (22x22 mm²) that were used for the samples were cleaned using a chemical protocol that contained the following reagents:

1. Ethanol 99,9% pure
2. H₂O (Milli-Q filtered)
3. Potassium hydroxide pellets (KOH)

20 g of KOH (Sigma Aldrich) pellets were weighed and added to 60 ml of ethanol. The mixture was stirred vigorously to dissolve the KOH pellets. The KOH-filled beaker was placed in an ultrasonic bath and sonicated for 5 mins. Two beakers were filled with 60ml of Milli-Q water and sonicated for 5 mins and one

of the beakers is left the bath for a further 5 mins. The cover slides are placed in a custom-made Teflon rack and submerged in the KOH- filled beaker and sonicated for 5 mins. The Teflon rack is removed from the KOH solution and is rinsed by dipping it in the Milli-Q water until the water runs smoothly off the cover slides without beading.

3.2.2 Single molecule sample preparation

0.5 mg of perylene dye powder was dissolved in a volume of 4 mL of toluene and sonicated for 10 mins at 20 °C to fully dissolve the powder, the concentration of the dye was calculated using equation (x) and found to be 0.50 mM. This sample was labelled as the stock sample concentration C_0 and from the stock sample solution a volume of 5 μ l was pipetted out and diluted with a volume of 4 ml of toluene in two stages to ensure that a very lowly concentrated solution. At each dilution stage, each sample solution was sonicated for 10 mins and at 20 °C. The third sample solution labelled as sample concentration C_3 with a concentration of 7.74 pM was calculated using equation (xi), were 100 μ l from this sample solution was spin coated onto a glass cover slide and used for single molecule microscopy measurements.

$$C = \frac{m}{m_r V} \quad (x)$$

C- concentration of solution, m- mass of solute, m_r - molar mass of perylene dye and V – volume of solvent.

$$C_0 = \frac{0.5 \text{ mg}}{252.316 \text{ g/mol} \times 4 \text{ ml}} = 0.50 \text{ mM}$$

$$C_3 = C_2 \frac{V_2}{V_3} \quad (xi)$$

$$C_3 = 61.93 \text{ nM} \times \frac{0.5 \mu\text{l}}{4 \text{ ml}} = 7.74 \text{ pM}$$

3.2.3 Polymer sample preparation and thickness measurements

Prior to embedding dye molecules in the polymer, a generic procedure to create polymer thin films was developed and the thickness of the films was determined using UV-Vis absorption measurements together with accompanying calculations. In this work the dynamics of polystyrene with molecular weight M_w of 35 000 g mol^{-1} (Sigma Aldrich) and poly (isobutyl methacrylate) with molecular weight M_w of 70 000 g mol^{-1} (Sigma Aldrich) were investigated. To produce thin films, 92.7 mg of polystyrene beads and 115.8 mg of poly (isobutyl methacrylate) beads were weighed on a digital mass meter and then dissolved in 4 ml of toluene separately. Both polymer solutions were dissolved further into two solutions and sonicated for

30 mins at 20 °C. The concentration of the polymer solutions was calculated using equation (xii) and found to be 0.40wt% and 0.75wt% for polystyrene and poly (isobutyl methacrylate) respectively.

$$\text{cwt\%} = \frac{\text{weight of solute}}{\text{weight of solvent}} \times 100\% \quad (\text{xii})$$

These polymer/solvent stock solutions were used to produce polymer thin films on the cover glass slides. Thin films were produced by dropping a predetermined concentration and volume of the polymer/stock solution on a rapidly rotating glass slide. This process is referred to as spin coating and it is well understood that the thickness of the film can be precisely controlled by choosing the appropriate spin speed. In order to determine the actual film thickness, the UV absorption of the polymer is used as a thickness measure. This is simple to understand as a thicker film would result in an increase in absorbance measured using the UV-VIS spectrophotometer. A volume of 100 μl of 0.4 wt% of polystyrene solution was spin coated onto a magnesium fluoride mirror at 640 rpm. Magnesium fluoride was chosen as it has a negligible absorbance at the desired absorption maximum of the polymers. Traditionally, using the Beer-Lambert Law the measured absorbance is equated to the molar absorptivity multiplied by the sample concentration and the optical path-length (here the thickness of the sample). However, the molar absorptivity for polymer films are not readily available and without knowledge thereof one cannot determine the thickness quantitatively. A convenient strategy to overcome this limitation, is to recognize that the absorption A must also be proportional not only to the thickness of the sample l but also to its density ρ (equation xiii).

$$A \propto \rho l \quad (\text{xiii})$$

The thickness of the spin coated polymer film is then determined using the densities of a liquid polymer solution and that of the solid spin coated polymer film. The method of thickness determination is given by the ratio of the absorbances for the liquid polymer Abs_1 to that of the solid thin polymer Abs_2 shown in equation (xiv).

$$\begin{aligned} Abs_1 &\propto \rho_1 l_1 \\ Abs_2 &\propto \rho_2 l_2 \end{aligned} \quad (\text{xiv})$$

The absorbance of a known mass and volume of a polystyrene liquid was measured in a standard 1 cm UV-vis cuvette at a selected peak wavelength of 260 nm. The absorbance of the spin coated 0.4 wt% polystyrene film was measured at the selected wavelength, with the assumption that the density of the spin coated polystyrene is the same as that of a bulk polystyrene film (Figure 11). The thickness of the solid 0.4 wt% polymer film on the magnesium fluoride mirror was determined using equation (xiv), since the only unknown is the solid film thickness l_2 and calculated as 941 nm.

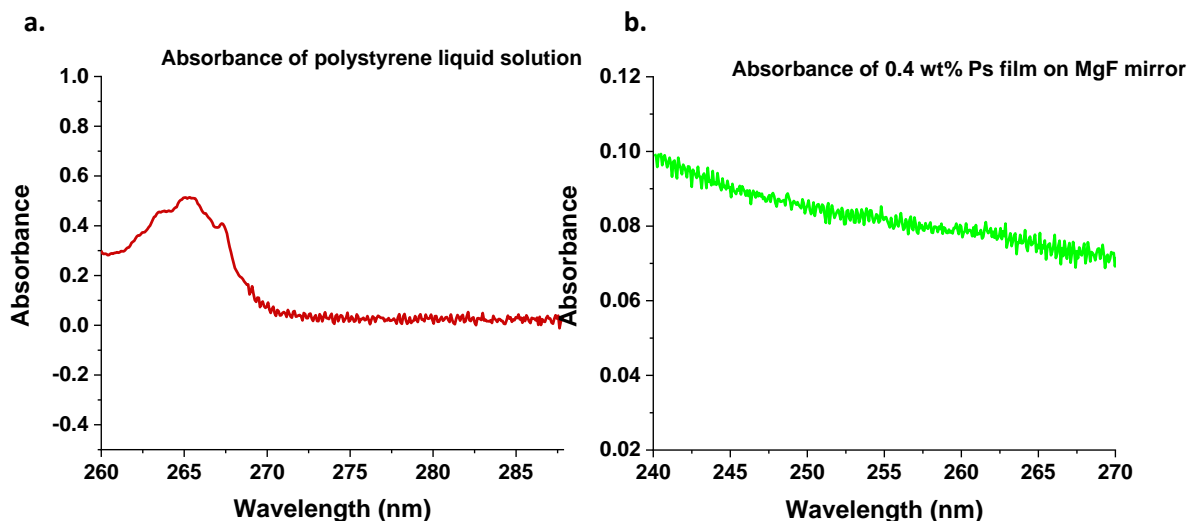


Figure 11. The thickness of polystyrene films is determined using the ratio of absorbance of liquid polystyrene solution (a) and that of a solid polystyrene film spin-coated on a MgF slide (b), where the absorbance is proportional to the density of the material and its length/thickness. The absorbance of the liquid polystyrene liquid solution was measured to be 0.5 and that of the polystyrene film 0.1.

The thickness of the polymer sample can be varied by changing the spin speed for spin coating [33]. The thickness of the film is related to the spin speed through equation (xv).

$$h \propto \omega^{-\frac{2}{3}} \quad (\text{xv})$$

h- thickness of sample and ω – spin speed.

The films that were used in this work were spin coated at a spin speed of 2000 rpm and thus the thickness is < 900nm. From dye sample solution, 5 μl , 1 μl was pipetted out and mixed with 200 μl , 300 μl of the polystyrene and poly (isobutyl methacrylate) solutions respectively and sonicated for 30 mins at 20 °C to thoroughly mix the two solutions. 100 μl from the mixed dye and polymer solution was spin coated onto a coverslide, the sample was heated up to 80 °C under vacuum for 5 hrs so as to evaporate any residual solvent remaining and also to remove any stresses and strains on the polymer film due to the spin coating procedure. This relaxed polymer film sample was then used to carry out single molecule microscopy measurements.

3.3 Setup characteristics

In this section the designed optical system is characterized using the image calibration factor which is used for determining the distance between single molecules. The localization precision is also used for system characterization, it is used to describe the limit to which a fluorescing point object can be located. Long term microscope stage position stability conditions are discussed, and these influence the ability of a microscope to maintain the selected focal plane over extended periods of time. Lastly the design of a custom-made heating stage used for heating the polymer film samples is described.

3.3.1 Image calibration

Image calibration is used to be able to distinguish in real space the distance between two single molecules. A 10 μm calibration gridded slide was illuminated with a halogen lamp from the microscope objective and an image was captured using the CMOS camera. The image was then processed using ImageJ, a horizontal cross-sectional line cut-out was drawn across the image to get an intensity profile of the gridded slide (in red), the resulting cross-sectional intensity profile. The full width at half height along the intensity profile (indicated in Figure 12) was 270 pixels. These 270 pixels in real space is equal to 10 μm , thus giving us a convenient calibration factor. The relationship between real space dimensions and CMOS pixel dimension is:

$$\mu\text{m: pix calibration factor} = \frac{10 \mu\text{m}}{270 \text{ pix}} = 0.037 \mu\text{mpix}^{-1} = 37 \text{ nmpix}^{-1}$$

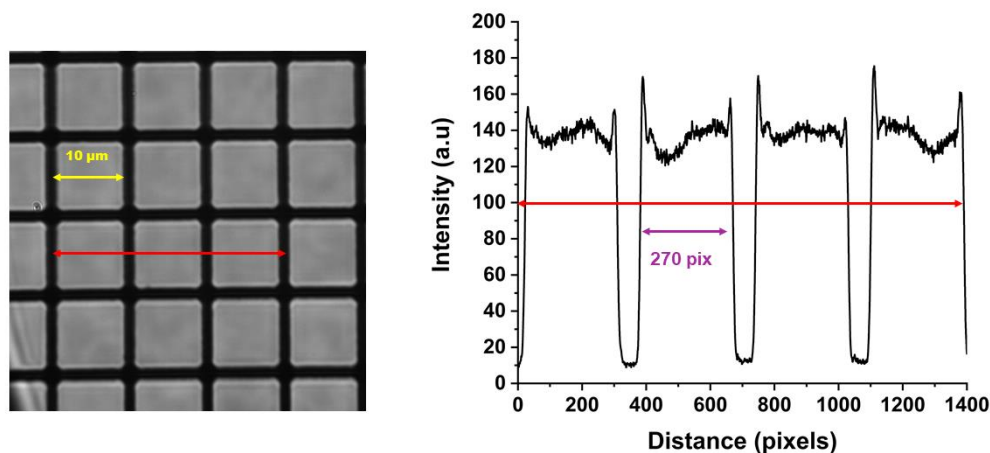


Figure 12. Image on the left shows the grayscale image of the calibration grid and on the right, the intensity profile resulting from cutting along a horizontal line drawn across the grid using ImageJ. 270 pixels counted on camera represents 10 μm in real space dimensions of the grid imaged.

The calibration factor helps in finding the distance between single molecules for instance if two fluorescing point objects are 20 pixels from one another, then the distance in real space between the two fluorescent single point objects is $20 \text{ pixels} * 37 \text{ nmpix}^{-1} = 740 \text{ nm}$.

3.3.2 Localization precision

The localization precision in single molecule resolved fluorescence microscopy is a measure which provides a simple yet intuitive way to determine the limit to which a fluorescing point object can be located. For single molecules, the localization precision is calculated as the standard deviation (σ_{LP}) of the loci x_i (position of maximum intensity for the single molecule) over a number N of captured frames (expression x_i).

$$\sigma_{LP} = \sqrt{\frac{\sum_{i=1}^N (x_{iI} - \bar{x}_I)^2}{N - 1}} \quad (\text{xvi})$$

N – number of frames, x_{iI} is the loci in frame i and \bar{x}_I is the mean loci over all frames.

Eleven individual fluorescent perylene dye molecules embedded in a thin polystyrene matrix were imaged over 100 frames and their loci found using Image J software, from which the localization precision was calculated in both X and Y directions using equation (xvi). The mean localization precision was calculated as $19.18 \text{ nm} \pm 10 \text{ nm}$ and $19.45 \text{ nm} \pm 9 \text{ nm}$ in X and Y respectively.

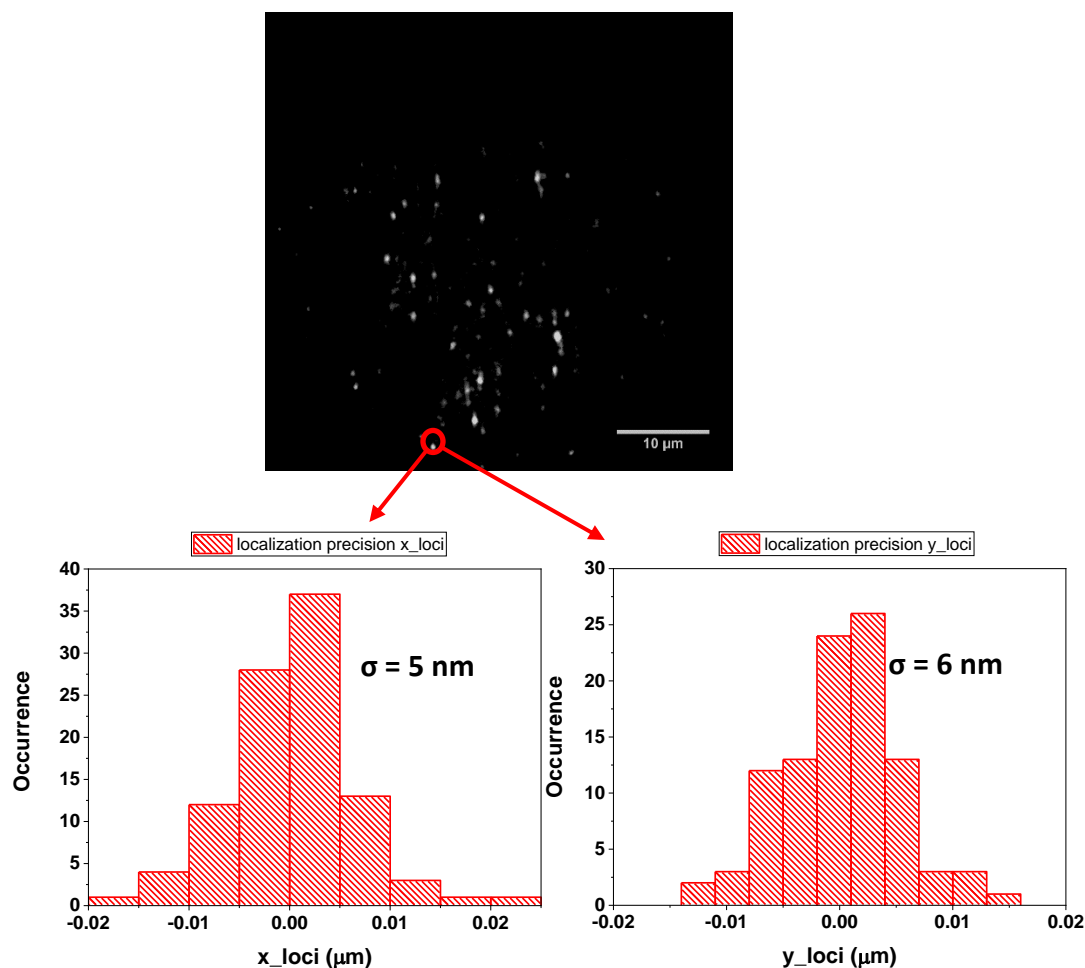


Figure13. Localization precision of single fluorescent perylene dye molecules embedded in polystyrene (circled in red) were imaged over 100 frames, camera exposure time of 500 ms and at a temperature of 17 °C. The loci of the individual emitters were used to calculate the localization precision in both the X $\sigma = 5 \text{ nm}$ (bottom left) and Y $\sigma = 6 \text{ nm}$ (bottom right) directions. The deviation in the localization precision is a result of the polymer chain nano-environment which is known to be complex as was studied by Tomczak et al [34].

3.3.3 Long term microscope stage position stability conditions

Mechanical microscope sample stage drift due to inappropriately torque placed on mechanical parts and thermal expansion due to varying thermal conditions influences the ability of a microscope to maintain the selected focal plane over extended period of time [35]. Therefore, the localization precision increases (x_{il} differs substantially from $x_{i,l}$ mean) by gradual changes of the sample focus especially when using high numerical aperture oil immersion objectives. The long-term mechanical stability of the fluorescence setup was thus determined through monitoring the fluorescence of a bright object. 2 μm fluorescent microspheres (SPHERO™ Fluorescent particles, Nile Red, High Intensity, 1.7-2.2 μm) were spin coated onto a glass cover slide, excited using the optical set up and the fluorescent signatures imaged. A total of 30 images were acquired, the acquisition time was set to 60 s with an external exposure trigger time of 100 ms to reduce photo bleaching the microspheres. To establish whether the objects loci differs from the mean loci and hence drifted, the images acquired were analyzed and the diffusion coefficients of the microspheres was obtained using an ImageJ plugin 'Particle Tracker' developed by Sbalzarini et al. The average drift of the microspheres over the 30 mins was found to be $2.04 \text{ nm}^2\text{s}^{-1}$ (Figure 14). From this measurement a conclusion can be drawn that the drift is negligible, as the acquisition time for the single molecule fluorescence in polymer films does not exceed 2 minutes which suggest that the diffusion due to stage effects is orders less than the typical diffusion coefficients measured in Chapter 4 ($> 500 \text{ nm}^2\text{s}^{-1}$).

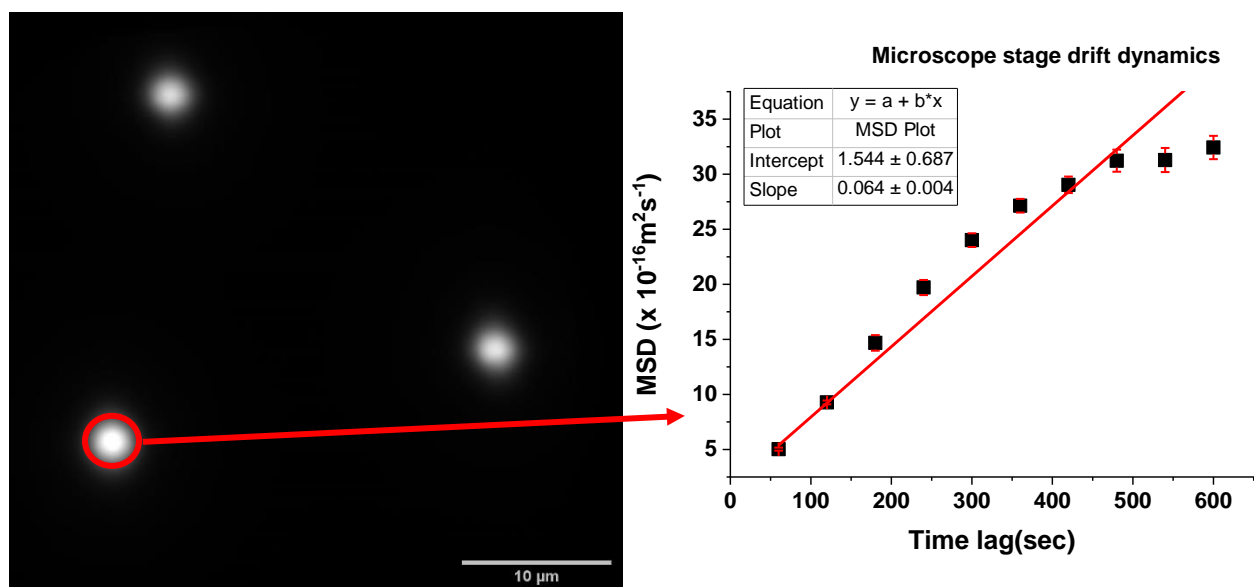


Figure 14. Image on the left shows three 2 μm fluorescent microspheres acquired over 30 mins and used to characterize the microscope stage drift dynamics. The stage drift dynamics are characterized using the diffusion coefficient of the microspheres extracted from the slope of the MSD graph (right).

3.3.4 Heating stage setup

A custom-made heating stage was designed and built. As has been mentioned in Chapter 2, polymer film dynamics are affected by temperature and these dynamics directly influence processing and the application of thin polymer films in various industries. In this research work, one of the main objectives was to study these polymer dynamics as a function of temperature and try explaining the complex condensed matter dynamics by studying the motion of single fluorescent probes embedded in them, as such the need for heating the polymer films arises. The polymer films were heated using resistive/Joule heating, where an electric current is supplied by a power supply and passed through a conductive indium tin oxide (ITO) cover slide.

The thermal energy supplied to the polymer films is caused by interactions between the electrons and the atomic ions from the ITO cover slide, that restrict the motion of the electrons as the voltage is increased. The voltage supplied to the ITO cover slide creates a potential difference between two points of the conductive cover slide and an electric field is created that accelerates the motion of the electrons in the direction of the electric field and giving them kinetic energy. These accelerated electrons collide with the ions of the cover slide, are scattered randomly and thus produce thermal energy.

The custom-built heating stage consisted of two polished aluminum sheets attached to a Thorlabs Nanomax moving platform, a conductive cover slide is placed onto the polished aluminum sheets using conductive silver paste (Figure 15). This paste ensured that an electrical current pass from one aluminum sheet to the other passing through the ITO layer. The heating circuit is essentially a series electrical circuit of the power supply and the ITO cover slide (resistor). As the voltage was varied, a thermocouple was used to measure the temperature at the surface of the polymer spin coated side of ITO cover slide at different areas to ensure uniform heating across cover slide and a graph of temperature against voltage was plotted to illustrate heating (Figure 16).

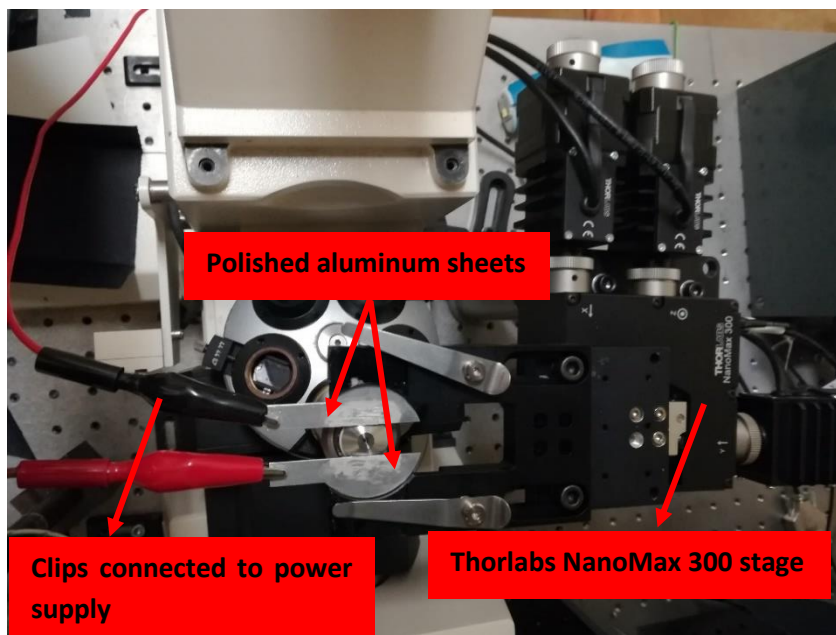


Figure 15. Heating setup used for heating polymer samples. The mechanisms employed to heat the samples is Joule heating, where a current is passed through the resistive ITO cover slide which then heats up as the charge carriers interact, collide and scatter from the ITO atomic ions, thereby producing thermal energy.

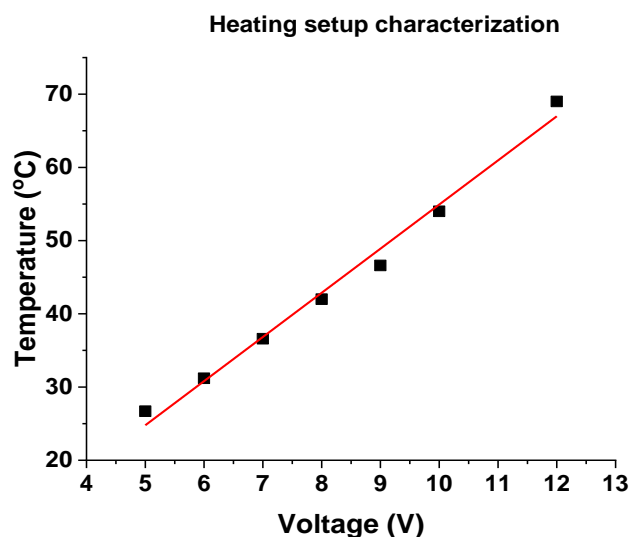


Figure 16. The graph shows that the heat energy is directly proportional to the voltage, current and thus an increase in voltage and current results in an increase in thermal heat energy.

Using widefield fluorescence microscopy in conjunction with the heating stage described above we were able to observe single fluorescent molecules embedded on cover slides and in thin polymer films environments, whilst varying the temperature. The use of single fluorescent molecules and monitoring their photo physical parameters when in polymeric nano-environments was further explored and described in much greater detail in Chapter 4. The dynamics of the polymeric environments and effects of heating up the polymer films at various temperatures were studied indirectly through widefield single fluorescence microscopy and the results thereof discussed in line with past literature, also discussed in the following chapter.

Chapter 4: Results and discussions

The fluorescence microscopy setup allowed the direct observation of single fluorescent probes. This was made possible through the careful preparation of the dye solution that had a concentration in the picomolar range, thus ensuring single molecules were sparsely spread out in the dye/polymer solution. The localization precision for the microscopy setup was in the range of 20 nm in both X and Y direction. As was mentioned in the previous chapter, the main goal of the research work was to study the local nano-environments of thin polymer films using the built fluorescence microscopy setup. Thin polymer films have become of paramount importance in various industries due to their complex behavior that has been noted as films are heated towards their service temperature, that is the glass transition temperature T_g . This complex behavior is a result of dynamic heterogeneities (T_g shifts) of thin films as compared to their bulkier counterparts and these dynamics directly influence the application of the polymer. A heating stage was built to heat the polymer films embedded with individual fluorescent probes at various temperature ranges to study the local polymer dynamics.

It is known from literature that single fluorescent probes are sensitive to their local nano-environment and minute changes in that local nano-environment, this was also shown in this section of the research work. Perylene bisimide (PBI) dye molecules were embedded in two different polymer matrices, polystyrene (Ps) and poly (isobutyl methacrylate) (Pibma) and their fluorescent signatures studied at 18 °C and at elevated temperatures. From the results of these measurements, a conclusion can be drawn that the current fluorescence microscopy setup is sensitive to polymer nano-environment and changes thereof. Static heterogeneities below T_g in polystyrene were investigated indirectly by observing the photophysical properties of PBI dye in an air environment and effect of embedding the PBI molecules in the Ps films. The results of these measurements showed photobleaching of the PBI dye molecules in both air environment and Ps environment with an effective a monotonic bleaching time of 8 ms in air and a photo bleaching rate that varied in Ps films as temperature was changed. The sensitivity of the setup facilitated the further investigations of the influence of temperature on thin polymer films below and near the T_g using the diffusivity of the individual fluorescent probes embedded in the thin Pibma films. From the results, discussions are made concerning the physical parameters that influence the diffusion of the fluorescent probes and how these parameters are linked to what is happening on the microscopic level of the polymer films, thus assisting in understanding dynamics such as β and α relaxation processes. Lastly the results are discussed in relation to bulk polymer models that have been used to try explaining the nano-environment of polymers as affected by temperature.

4.1 Polymer relaxation processes below T_g

Perylene dye molecules were embedded in two different polymer matrices, poly (isobutyl methacrylate) (Pibma) with T_g at 55 °C and polystyrene (Ps) with T_g at 100 °C (structures in Figure 17). The nature of the polymer is known to influence the dynamics of the individual fluorescent probes [14] and this was also shown in this research work. Both polymer samples were imaged under the same conditions, same exposure time (200 ms), the same laser fluence of $870 \mu\text{Wcm}^{-2}$ used for excitation and same temperature conditions (18.5 °C and 43.5 °C). Image frame sequences show molecules that appear and disappear caused by either photoblinking or photobleaching due to fluorescence quenching from interactions between the dye molecules, molecular oxygen and the polymer film (Figure 18).

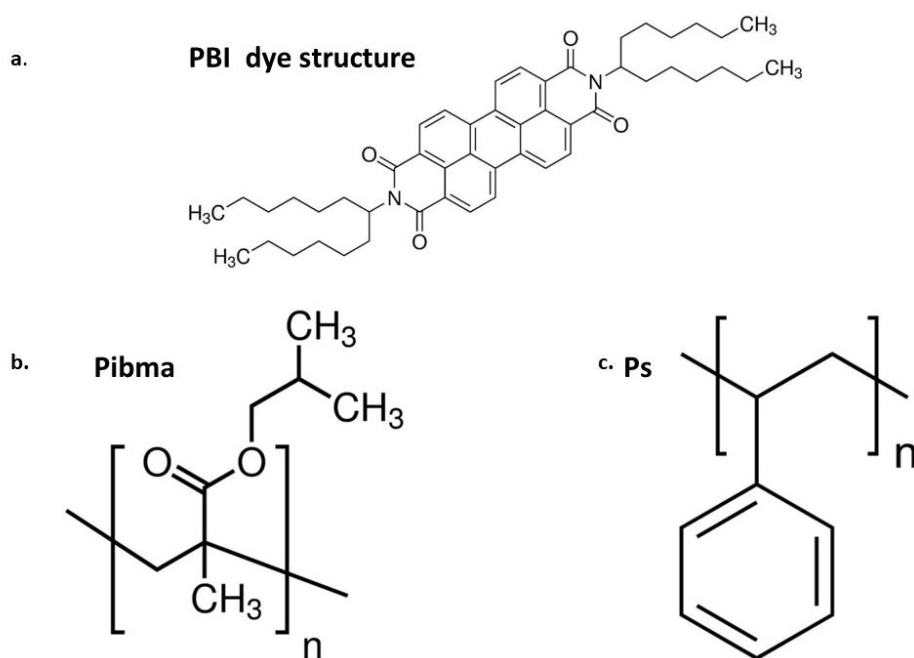


Figure 17. (a) The structure of the PBI dye molecule that was embedded in two different polymer environments. The polymers that were used in this research work are Pibma with glass transition temperature of 55 °C (b) and Ps with a lower glass transition temperature of 100 °C (c).

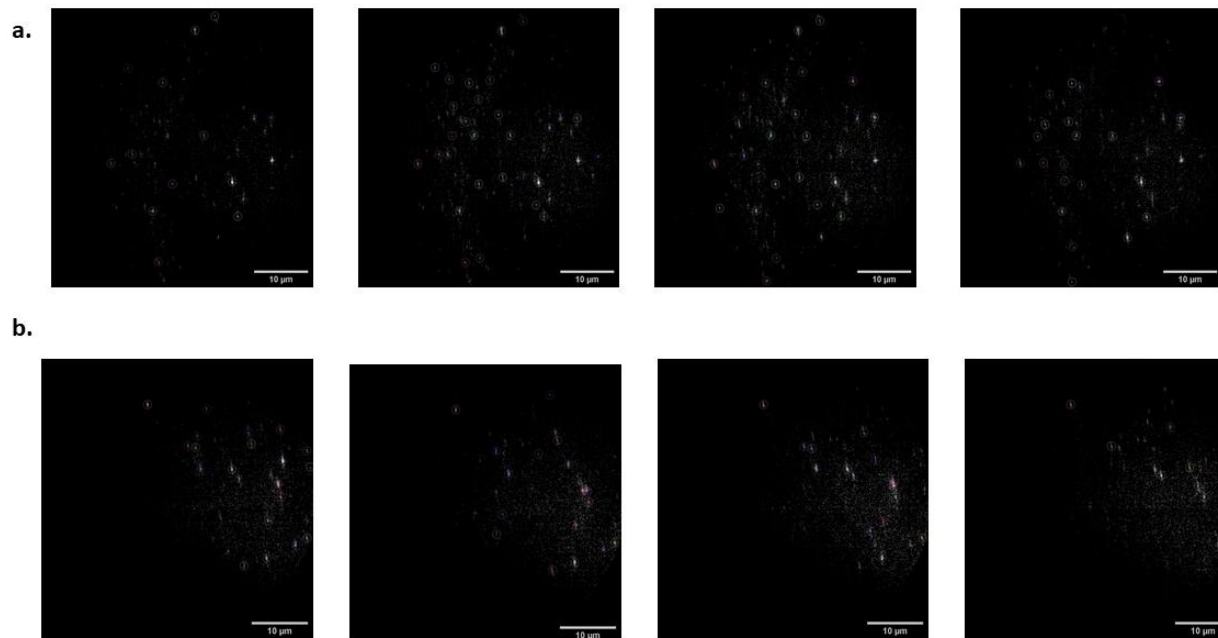


Figure 18. Image sequences of PBI dye molecules embedded in a Pibma (a) and Ps (b) film at an exposure time of 200 ms and 18.5 ° C. A notable difference between the two polymers on the fluorescence emission of PBI is the number of observable single molecules and the photobleaching of PBI molecules in Ps film.

The number of molecules in each frame were noted as a function of time for both the polymer films. The poly (isobutyl methacrylate) film images showed that the number of single molecules in each image relatively stays the same with fluctuations due to photoblinking, however for the polystyrene film some of the molecules permanently disappeared as a function of time due to photo bleaching and others were noted to photo-blink (Figure 19).

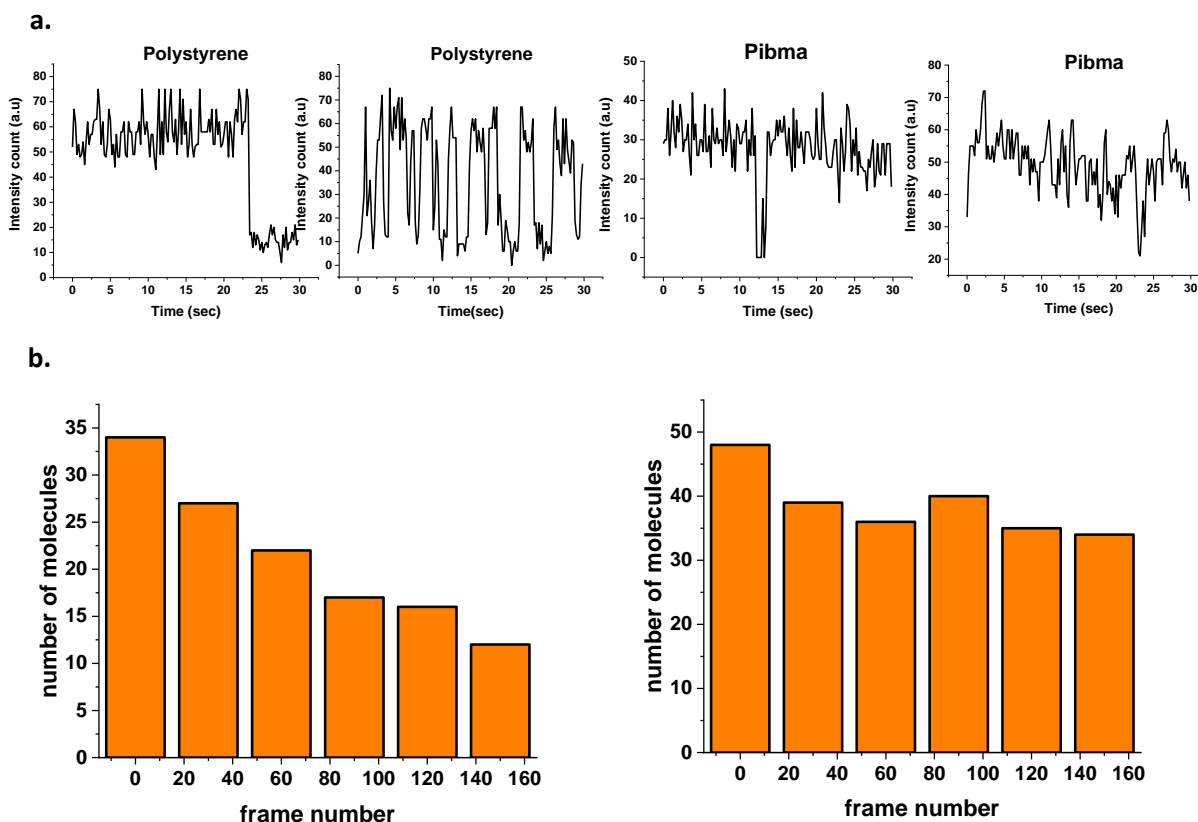


Figure 19. (a) Insert show the typical blinking behavior of single molecules in the thin polymer films. (b) Influence of polymer environment to single fluorescent molecules emission. From the Ps film, the individual fluorescent probes were noted to photo blink and most photo bleaching as a function of time. The Pibma film showed the number of fluorescent probes to relatively stay the same across each image frame and photo blinking was observed.

Far below the T_g the molecular chain mobility is limited or frozen and as a result the distributions of the diffusion coefficient of the probe molecules in the polymer is narrow (Figure 20). The mobility or lack thereof of the polymer chains is determined by tracking the diffusion of the individual probe molecules. By studying the fluorescence emission patterns and the single molecule motions in the nano-environments of polymers enables one to report on the polymeric dynamics that are coupled with the relaxation processes of polymers. From these results it was shown that for both polymer matrices had an influence on the fluorescence of the perylene dye. Comparing the average diffusion coefficient found by Flier et al of $30 - 50 \text{ nm}^2\text{s}^{-1}$ [4], [9] it is clear that in the limited time window no appreciable dynamics occurred we only consider the probe diffusion. However, the photo bleaching and blinking which varies substantially (Figure 19) in the two films provides a glimpse into the nano-environment. A common cause for the varying photophysical behavior includes probe and monomer re-orientation and the polymer free volume variations [5], [14], [36]. Deeper investigations into the origin of the stark difference between the

photostability on the probe in the two different polymer films are currently outside the scope of this project.

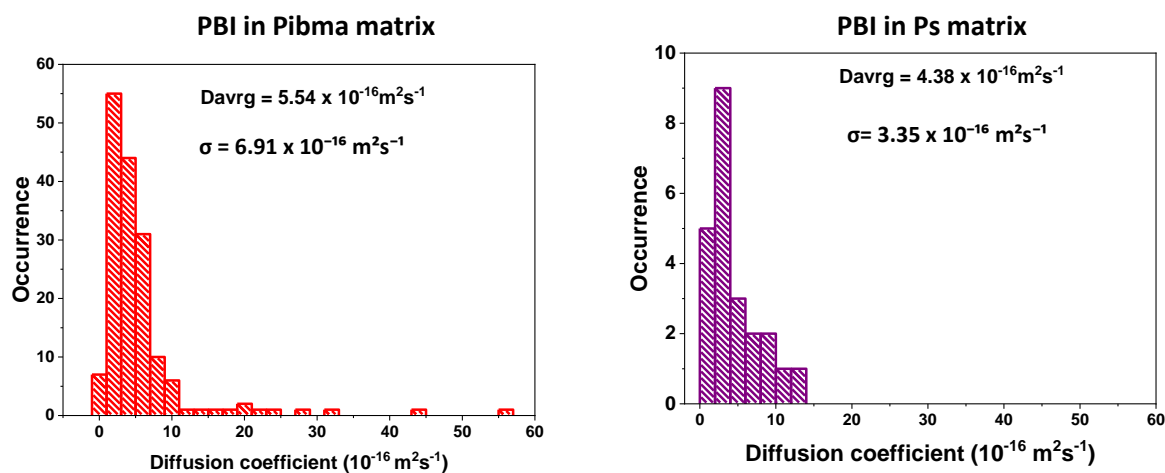


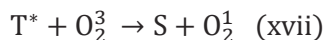
Figure 20. Narrow distributions of the diffusion coefficients of PBI in Pibma (on the left-hand side) and Ps (on the right-hand side) thin films imaged at 18.5 °C show that far below the glass transition temperature the polymer chains and segments are rigid. The rigidity of the polymer chains and segments means reduced free volume distributions in the polymer or the caging effects that hinders motion of small probe molecules within the polymer film at very low temperatures below T_g [37].

4.2 Static heterogeneity for PBI in Ps film below T_g

PBI dye molecules embedded in Ps films did not show any visible translational diffusion and were effectively immobilized in the polymer matrix. Our widefield optical setup was successful in observing single molecules however its application to study polystyrene slow dynamics at the temperature range of 18.5 – 43.5 °C was limited. Static heterogeneities in polystyrene film were studied indirectly by observing the intensity traces of PBI dye spin-coated on an ITO cover slide and comparing the intensity traces of the same probe molecule embedded in polystyrene. It is known and has been mentioned in Chapter 2 that the fluorescence emission of single molecules is extremely sensitive to changes in their nano-environment, thus if the photophysical properties of the probe molecule fluctuate in time when in two different environments then these fluctuations should be a result of dynamics of the probe environment.

The fluorescence emission intensity traces of PBI dye molecules embedded on a plain ITO cover slide showed fluorescence quenching at 18.5 and 43.5 °C (Figure 21). The fluorescence bleaching can be explained by photo-chemical processes caused by molecular oxygen that is known for photobleaching via triplet state excursion. The triplet state lifetimes are dependent on the concentration of molecular oxygen. Triplet – triplet state annihilation mechanism causes formation of singlet state oxygen species between the dye and the molecular oxygen [38] and single molecules in the excited triplet state exhibit high degree of chemical reactivity and react with the molecular oxygen, which is then excited to a reactive

singlet state thus quenching the fluorescence emission of the PBI dye through photo-chemical oxidation (equation xvii).



By changing the environment of the PBI dye molecule and embedding it in the Ps film the fluorescence emission is also expected to change. Observations from our measurements showed photobleaching and an increased average number of molecules observed when the PBI was embedded in the Ps film as compared to measurements of PBI in air. These changes observed can be qualitatively explained as reduction of oxygen concentration in the polymer film and a lower oxygen concentration means the probability of oxygen-probe interaction is minimized, therefore lowering probability for photo bleaching (Figure 22). A minor drawback from our system is the inability to give quantitative information regarding the triplet lifetimes on the intersystem crossing yield which have been reported to be in the range of a few microseconds [39], shorter than the integration time of our system (200 ms).

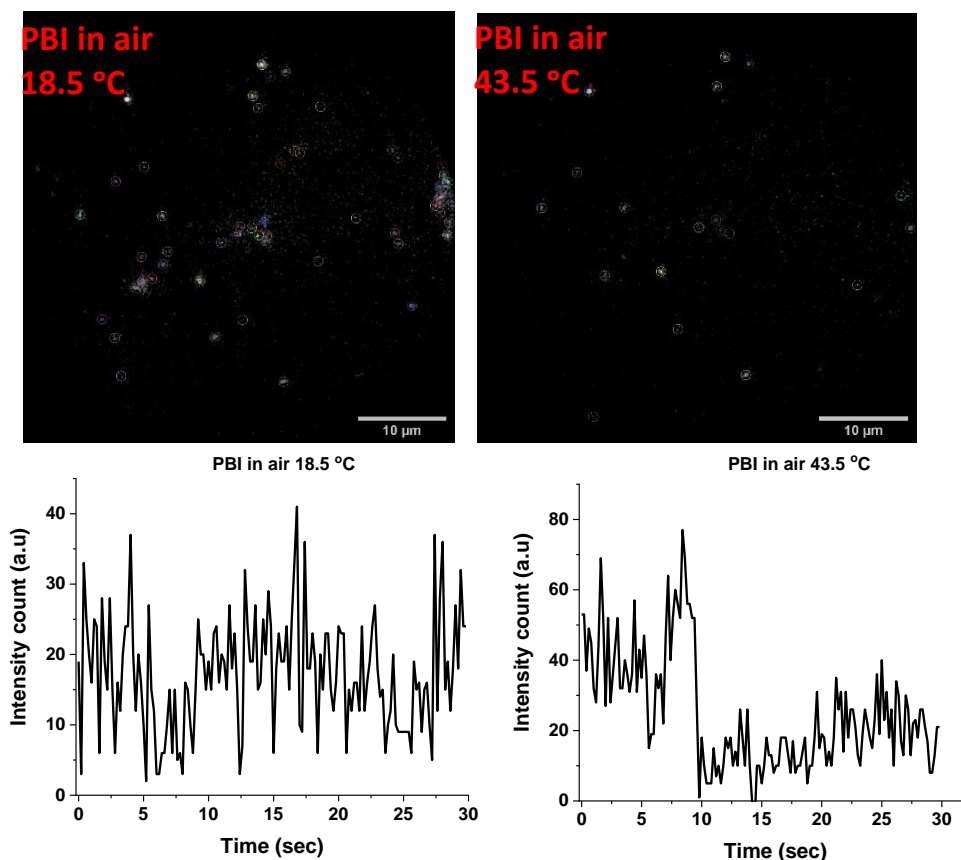


Figure 21. Static heterogeneities of polystyrene were studied by observing the photo physical changes of PBI in air as a function of temperature. Photo blinking and photo bleaching of single molecules was observed with increased photo bleaching for PBI in air.

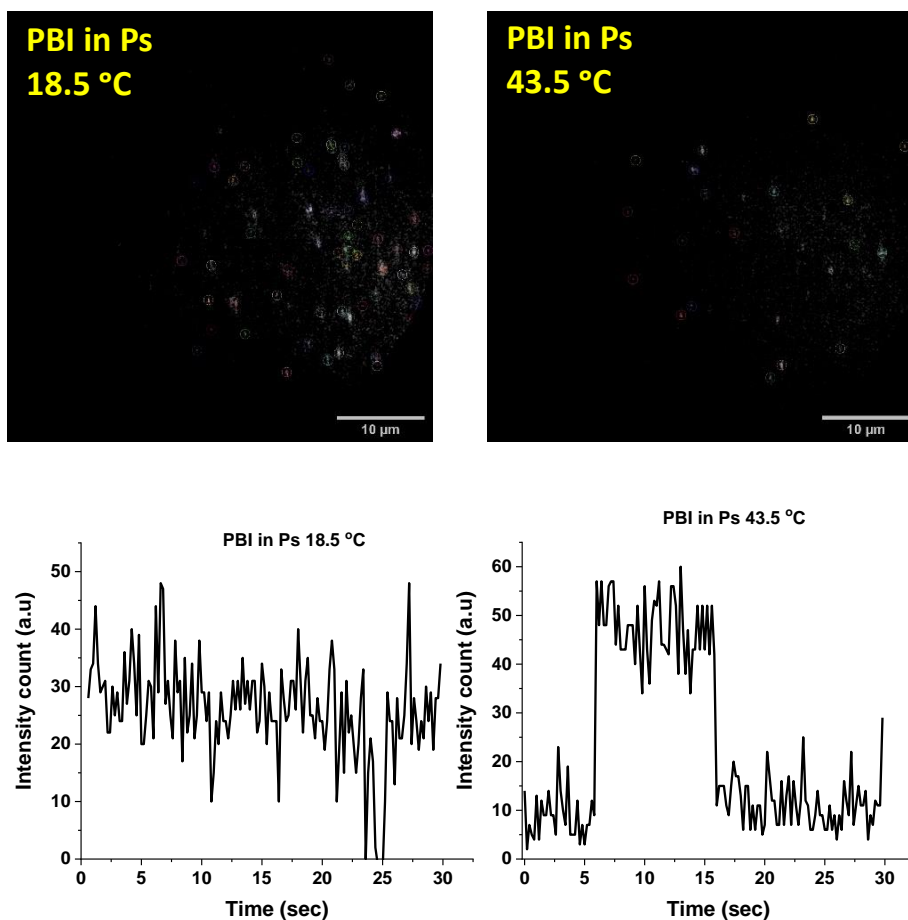


Figure 22. Static heterogeneities of polystyrene were studied by observing the photo physical changes of PBI in a Ps film as a function of temperature. The number of observed single PBI molecules in a Ps film increase as compared to single PBI molecules on a plain ITO cover slide.

An effective photobleaching rate of the dye molecules in air and in the polystyrene film matrix was found by assuming a single exponential function equation (xviii). The results show that the fluorescence microscopy setup used in this research work was sensitive to nano-environment changes and local density fluctuations in Ps below T_g for the PBI embedded in Ps. It has been studied by [40] that temperature affects the rigidity of a polymer and photobleaching can be used to probe the T_g for PVA (Poly vinyl alcohol). A change in temperature influences the mobility of the chain segments of the polymers, as the temperature is increased and the free volume redistribution in the polymers also changes thus influencing the fluorescence of the perylene dye molecules and the diffusion of the molecular oxygen within the polymer film (Figure 23). As the temperature is increased the effective bleaching rate of the PBI in Ps film reduces due to static heterogeneities in the polymer film caused by density fluctuations of the polymer film and for the PBI in the air the effective bleaching rate is constant as the temperature is increased.

$$\ln N = -kt + \ln C \quad (\text{xviii})$$

N is the number of single molecules across each image frame, C is a constant, k is the effective photobleaching rate and t is the time.

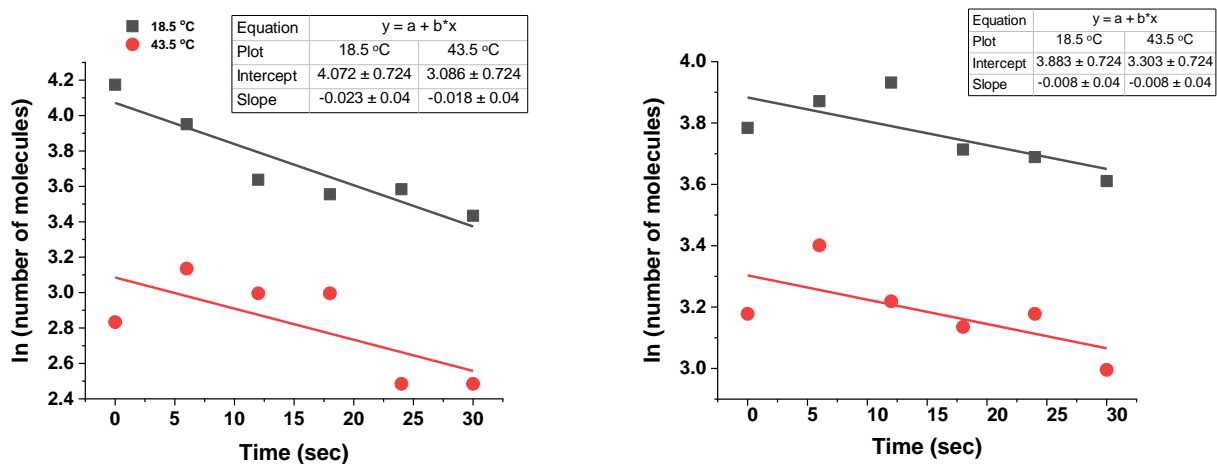


Figure 23. The effective photo bleaching rate reduces as temperature is increased for PBI in Ps film 23 ms to 18 ms for 18.5 °C and 43.5 °C respectively (on the left-hand side). The effective photo bleaching rate PBI in air is approximately constant ~ 8 ms for both temperatures (on the right-hand side). The effective photo bleaching rate was extracted from the slope of the linear fit graph.

A reduced average fluorescence intensity traces was observed from the Ps films and photo bleaching with an increase in temperature. This reduced intensity trace and photobleaching may be a result of reorientation of probe molecules embedded in the polymer matrix causing fluorescence fluctuations as temperature is increased (Figure 24). It is well established that rotational diffusion of probe molecules in polymer matrices correlates with segmental dynamics of the polymer [15]. However, using the current optical set-up, the reorientation of perylene dye molecules in the polystyrene film could not be conclusively established at these temperature ranges because of a small sampling. To obtain full information about the molecular orientation of PBI in Ps below T_g , a larger sampling is required and more sophisticated and dedicated optical setups with advanced pattern analysis is required such as using a SLM (special light modulator) to monitor the fluorescence intensity fluctuations and patterns if the polymer host allows the probe to rotate [41].

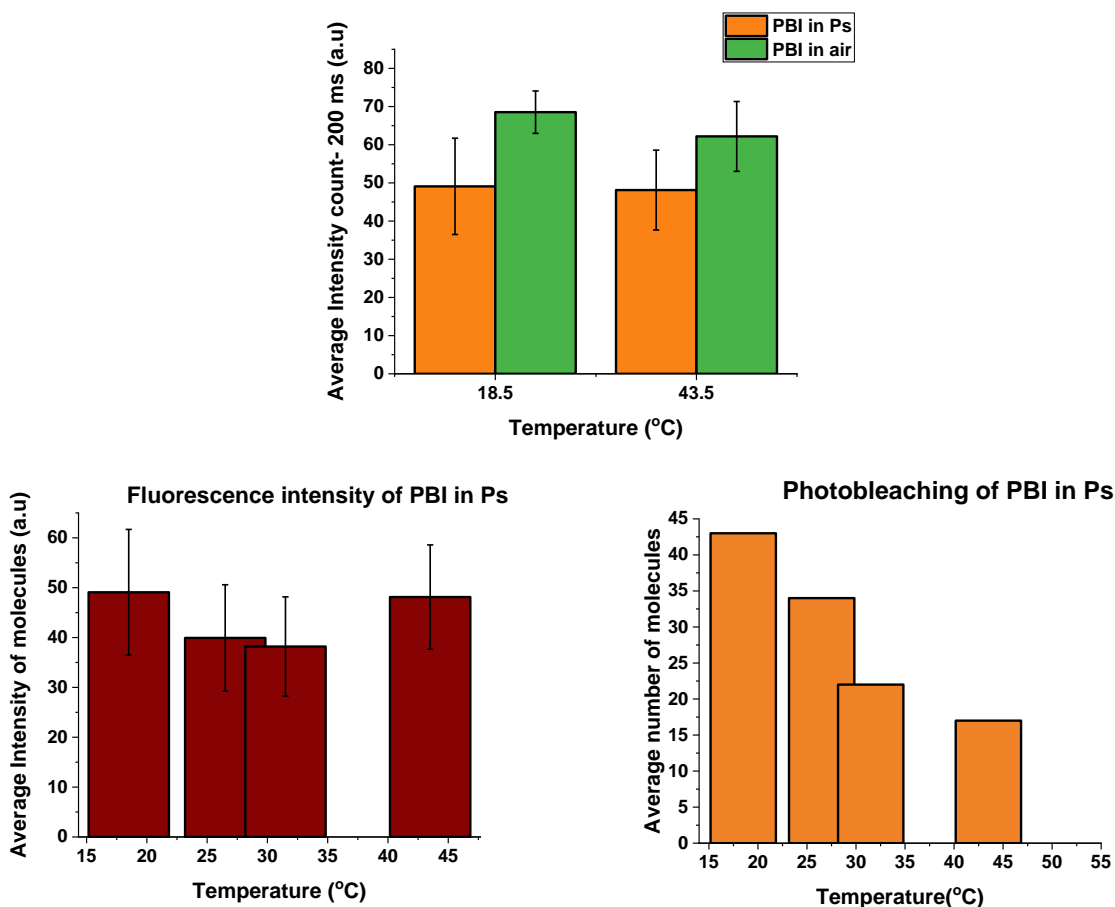


Figure 24. The average intensity count for PBI in Ps film was lower than that of PBI in air (top graph). Fluctuations in the average intensity trace of PBI as the temperature is increased (left) is attributed to the static heterogeneities within the polymer film that include different amounts of free volume distribution, enhanced surface interfaces because of the thin film and local density fluctuations of the polymer chain segment structure. The excited PBI probe molecule fluorescence emission was influenced by the interactions between the polymer film and the amount of oxygen that could diffuse through the polymeric film as the temperature is increased these interactions also increased and contributed to the photo bleaching of PBI dye molecules in the Ps film (right).

Thus, the reduction in fluorescence intensity of the perylene dye may be assumed to be a cause of the interactions between the probe molecule and polymer host. J Pawley [42] hypothesized that if a dye has a high quantum yield for inter-system crossing, a significant number of the dye molecules will cross from a singlet excited state to the long-lived excited triplet state (millisecond time scale) and this process allows the molecules to interact with their environment for much longer times. The excited PBI molecules in the triplet state can also react directly with the polymer and this result in the deactivation of the fluorophore. The perylene bisimide dye used is electron deficient and may have reacted with polystyrene by intermolecular electron transfer and forming a radical of the perylene dye that fluoresce less [43], [44].

At low temperatures it is known that polymer chain segments are immobile, however these segments form cages that rattle/vibrate and as temperature is increased, the chain segments vibrate more as they gain thermal energy thus increasing more interactions between the perylene and the polymer matrix forming more dark state perylene radicals resulting in the reduction of fluorescence intensity of dye molecule as temperature is increased. The increased photobleaching of PBI in Ps films with increase in temperature may be due different amounts of free volume available for the oxygen to diffuse in the polystyrene film. It has been reported by [45] that the diffusion of oxygen at room temperature in polystyrene is $\sim 2 \times 10^{-11} \text{m}^2 \text{s}^{-1}$ and average diffusion coefficient of PBI in Ps from this work is $4.38 \times 10^{-16} \text{m}^2 \text{s}^{-1}$ hence increasing the temperature increases the free volume within the polymer and allows more oxygen to diffuse and interact with the PBI molecules and only the rigid parts of the polymer can slow down the diffusion process of the oxygen [46].

4.3 Single molecule diffusion of PBI in Pibma below T_g

PBI dye molecules embedded in a Pibma film showed translational diffusion in the temperature range 18.5 – 43.5 °C. Tracking of the PBI fluorescent probes was done using an ImageJ plugin developed by [47]. An assumption is made that the probe molecules are random walkers, the plugin extracts sets of space co-ordinates $\{x_i, y_i\}$ based on the loci of the probe molecules at each observation time t (Figure 25b). The single molecule trajectories are then obtained from which the mean square displacement (MSD) (Figure 26) at each frame integration time lag δt is calculated (equation xix)

$$\langle (\Delta r)^2 \rangle = \langle (x_{i+n}(t + \delta t) - x_i(t))^2 \rangle, \langle (y_{i+n}(t + \delta t) - y_i(t))^2 \rangle \quad (\text{xix})$$

x_i, y_i are the loci for the random walkers, i ranges from 1 to $N-n$, N is the number of random walkers and n takes on values 1,2,3.... $N/2$.

Using Einstein's diffusion theory in 2D [48], the diffusion coefficients of the single molecules is obtained from the MSD slope (equation xx)

$$\langle (\Delta r)^2 \rangle = 4D\delta t \quad (\text{xx})$$

D is the diffusion coefficient.

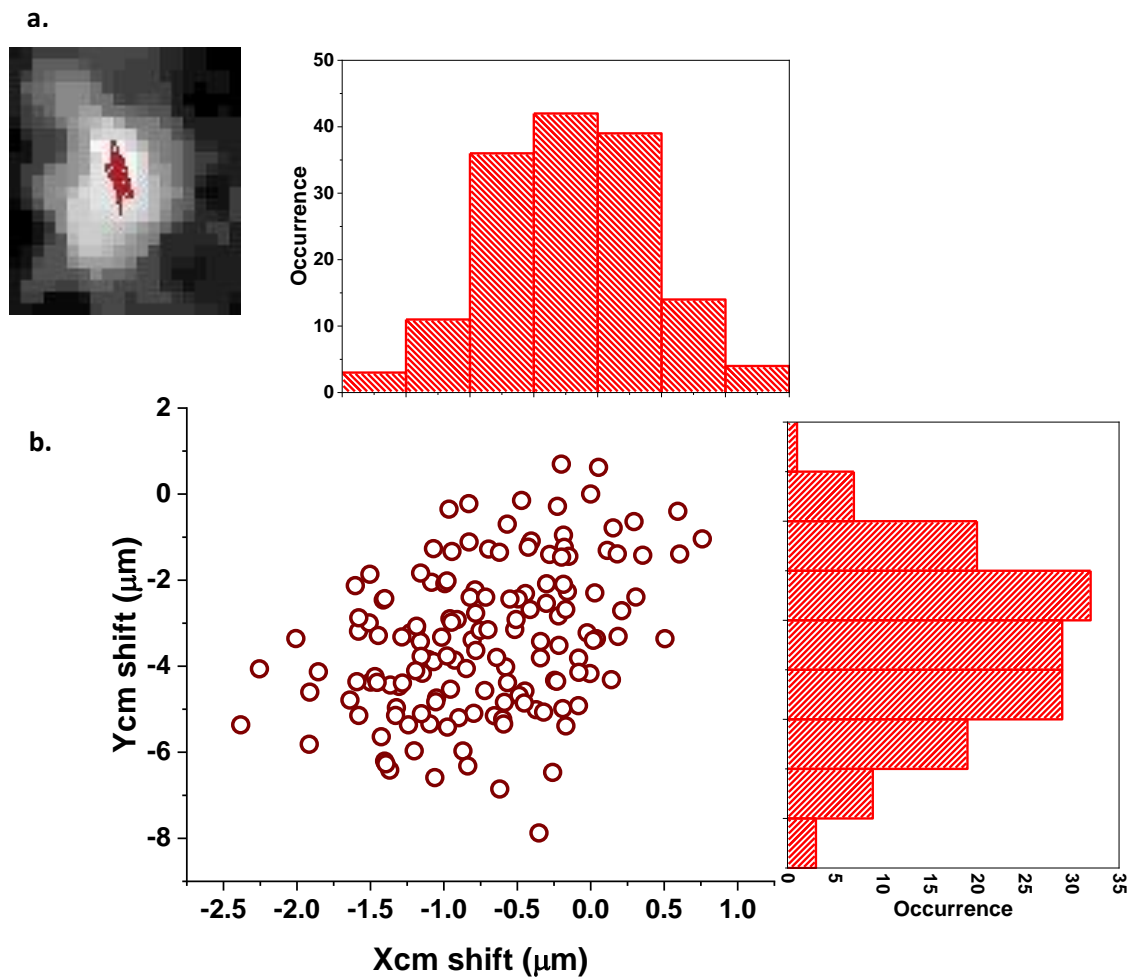


Figure 25. a) Zoomed in image of individual fluorescent molecule, the red pattern is the trajectory length indicating movement of the molecule. b) the loci position shifts from the initial start coordinate illustrate how the molecule moved in the x and y directions, movement is isotropic from the histogram distribution and can be assumed to be Brownian.

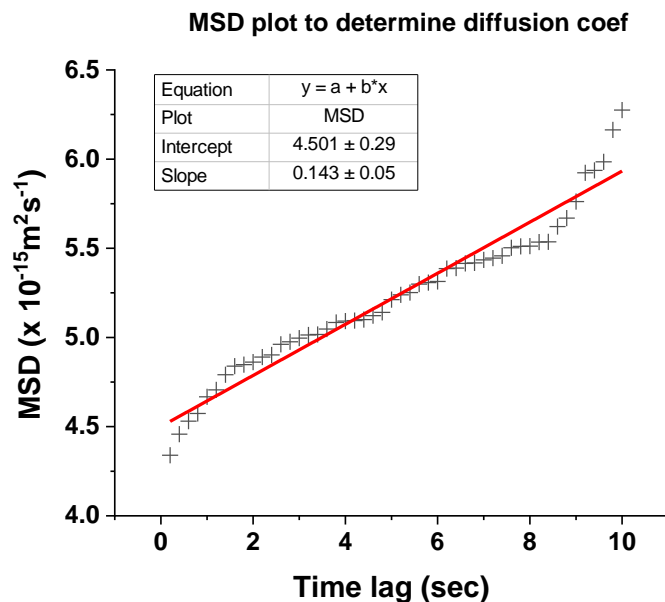


Figure 26. By tracking the molecule movement in the polymer, the mean square displacement is extracted at each time lag of 200 ms and from which the slope of the MSD plot gives the diffusion coefficient of an individual PBI in Pibma film.

Chain mobility of Pibma films was further studied by following the diffusion of PBI in the films at different temperature ranges. From the MSD plots, the diffusion coefficients of the PBI was determined and the distribution of the diffusion coefficients at the different temperature ranges plotted. The motion of the PBI probe molecules is influenced by the nano-environment it is in and therefore any changes in the surroundings influences the diffusion process. As has been mentioned in Chapter 2, at low temperatures motion of polymer chains is through cooperatively rearranging regions and local free volume is minimal thus the PBI tracer molecule motion shows a narrow diffusion coefficient distribution. An increase in temperature has an effect of increasing chain motion of the polymer, thus the local free volume of the polymer chains increases allowing the tracer molecules freedom to move within the cooperatively rearranging regions. However, these cooperatively rearranging regions are inhomogeneous, thus the motion of the PBI molecules is also inhomogeneous as observed from the standard deviation of the diffusion coefficient with increase in temperature (Figure 27).

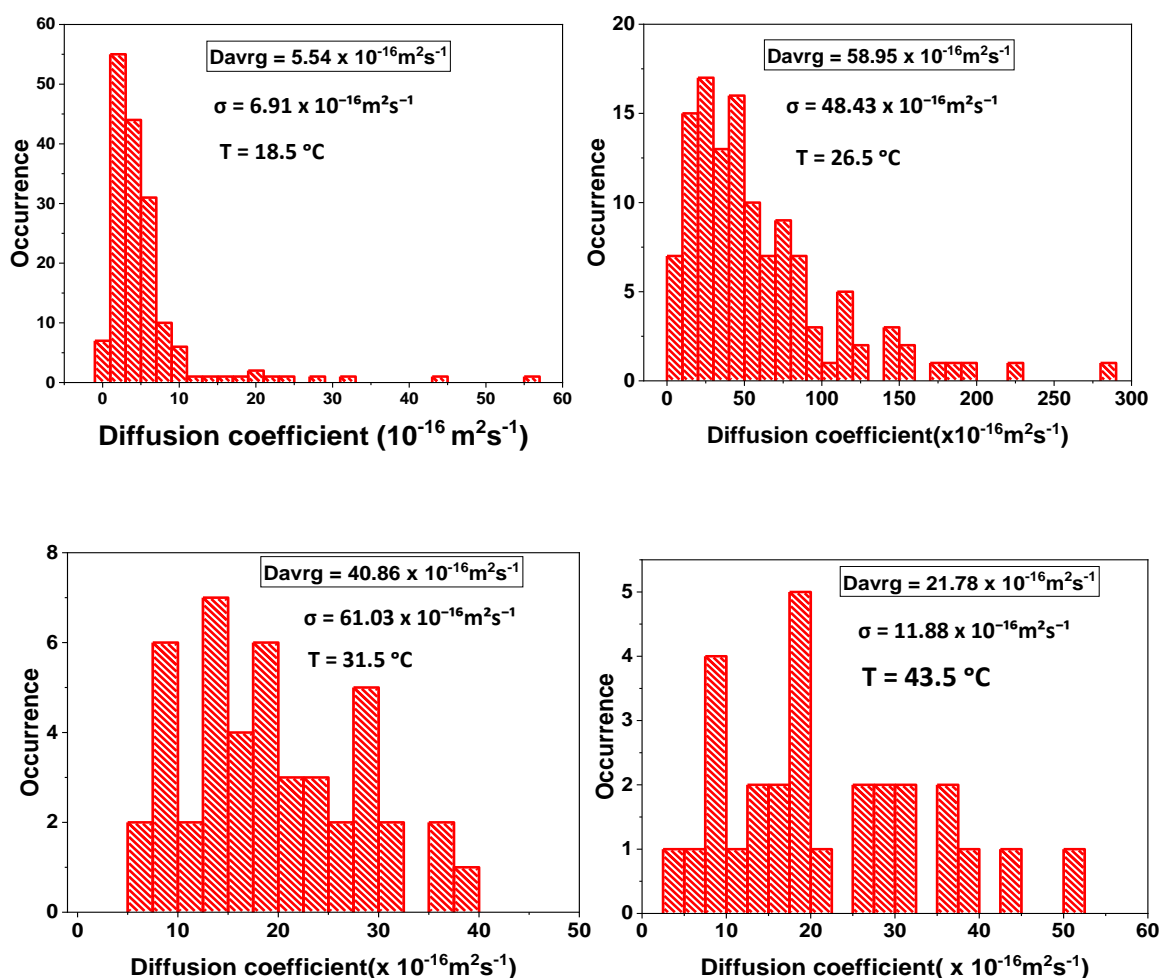


Figure 27. Diffusion coefficients of PBI in Pibma at four different temperature ranges indicates that as the temperature is increased the standard deviation of the diffusion coefficients increases due to the heterogeneous cooperatively rearranging regions. As the T_g for Pibma is slowly approached the translational diffusion of the PBI reduced.

For bulk polymers, the viscosity temperature dependency predicts that the diffusion coefficient of single molecules is expected to follow the Stokes-Einstein relation equation (xxi), however this law fails to determine the viscosity of the Pibma films used in this work. The Stokes-Einstein diffusion relation is only valid if the probe molecule size is larger than the radius of gyration of the polymer film used and in the case of this work PBI size was $d \sim 0.82\text{ nm}$ and radius of gyration for Pibma 2.14 nm [49].

$$D = \frac{k_b T}{3\pi\eta d} \quad (\text{xxi})$$

D is the diffusion coefficient of a particle of diameter d at a temperature of T , k_b is the Boltzmann constant. The viscosity η is a consequence of the micro dynamics of the environment the particle is in.

The viscosity temperature dependence of polymers is also expected to follow the Vogel-Fulcher law, thus if the α -relaxation process is being probed by the individual molecule, then its diffusion coefficient is also expected to follow the Vogel-Fulcher law, however this dependence could not be determined from the diffusion coefficients data. The diffusion coefficients do not follow the Vogel-Fulcher law due to the heterogeneities in the Pibma film which also cause different diffusion coefficients at each temperature measurements. As temperature is increased the standard deviation of the diffusion coefficients also increases until > 40 °C, where the translational diffusion processes are known to slow down (Figure 28). The slow down of the translational diffusion processes as T_g is approached (Pibma $T_g = 55$ °C), also observed by Nikodem et al [34], may be explained as due to the onset of large increase in viscosity of the polymer chains as T_g is approached thus hindering the translational diffusion processes.

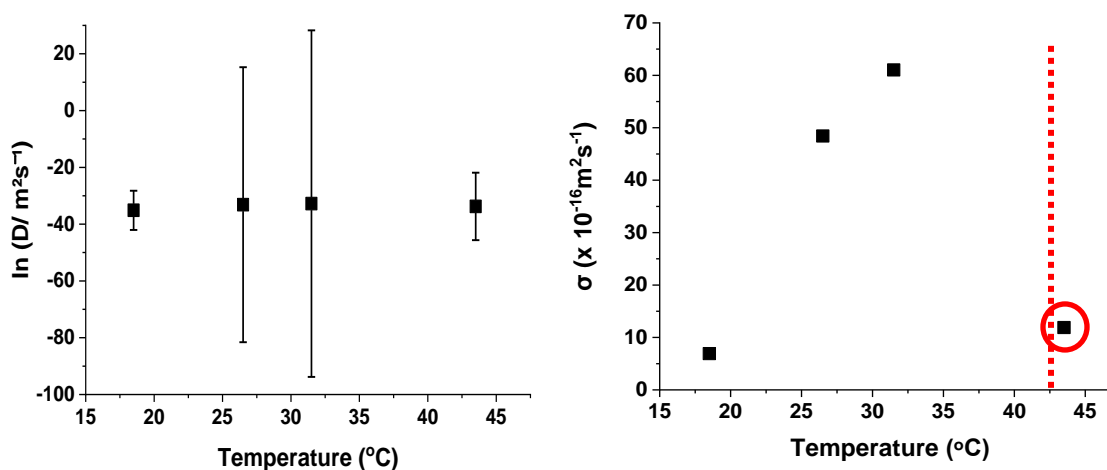


Figure 28. The Vogel-Fulcher law fails to describe the viscosity temperature dependence of the diffusion coefficients of PBI molecules in Pibma due to heterogeneities in the thin film as shown in the plot of $\ln(D)$ against temperature (left). A plot of the standard deviation of the diffusion coefficients illustrates the increase of heterogeneities as the temperature is increased until the approach of T_g of Pibma (55 °C), where the translational diffusion processes are slowed down (right).

The widefield fluorescence setup used in this research work enabled the observation of heterogeneities that would have otherwise been obscured in bulk measurements. These heterogeneities are a result of thin polymer films that influence the effects at the polymer-air interface such that a larger volume of the surface layer assists the mobility of single molecules at the polymer-air interface thus increases translational motion. Below and near T_g , the polymer chains do not have enough free volume to move about, however their motion is through cooperatively rearranging regions. The Adam-Gibbs model has been widely used to describe the cooperatively rearranging regions of polymers and how this movement is different at different relaxation processes in polymers.

The heterogeneities observed in our experiment can be explained as follows:

i) Below T_g , the CRR are immobile, however these regions vibrate and rattle against each other and the relaxation processes associated with this motion is the β -relaxation. Small molecules embedded in the polymer film experiences a ‘caging’ effect from the vibrational motion of the CRR. As temperature is increased, the caging effects are slowly reduced as the number of cooperatively rearranging regions are also reduced thus enabling the diffusion of small molecules within the film. Further increasing the temperature breaks the caging effects and allows increased diffusion of the probe molecules across the polymer nano-environment (Figure 29).

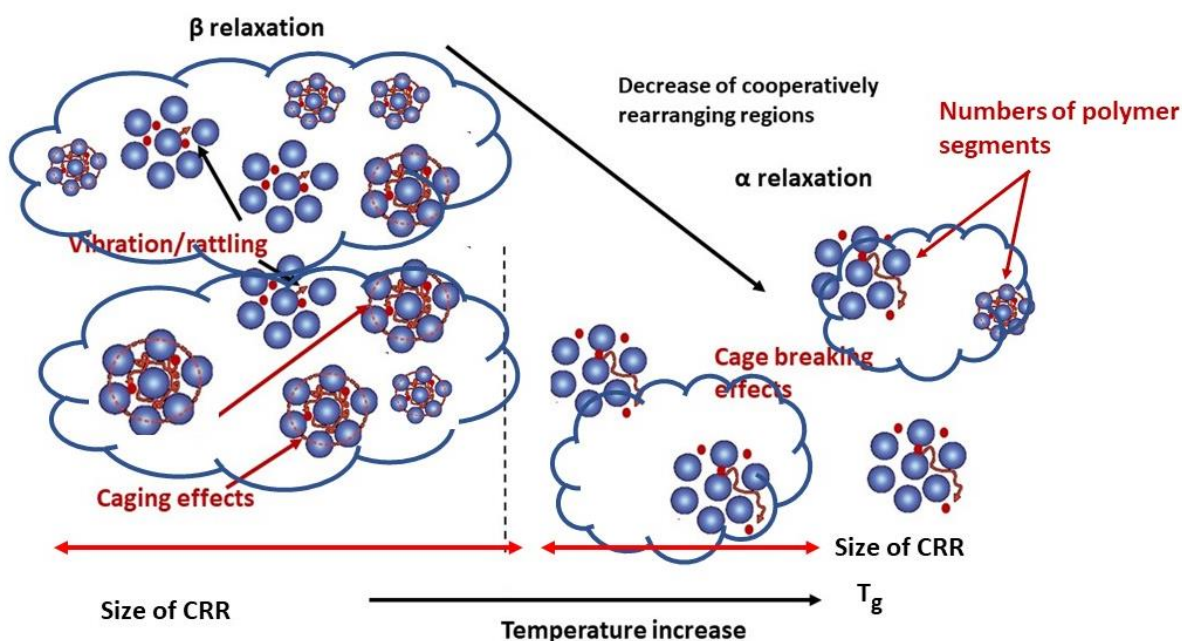


Figure 29. Cooperatively rearranging regions within a polymer have been said to cause a caging effect on probe molecules embedded in the polymer film. At low temperatures below the T_g of a polymer film, each size of the CRRs is large and the number of the polymer segments large and motion of the regions is through vibrations which are coupled to the probe molecules and the relaxation process associated with this motion is the β -relaxation. As the temperature is increased towards T_g , the size CRRs reduces and the number of polymer segments within the CRRs reduces hence breaking the caging effect on the tracer molecules [25], [34], [50]. The cage breaking effect enhances the diffusion of the probe molecules within the polymer film and the relaxation process associated with this motion is the α -relaxation process.

Our optical setup could not probe the β -relaxation process because the typical length scale $\ll 1$ nm [51] was beyond our observation scale of 19 nm from the localization precision. We could not determine the size of the CRRs, which was determined to be 5 nm by Ellison et al [52], also due to the system's localization precision of 19 nm. Even though the optical setup could not probe individual heterogeneities caused by each cooperative rearranging region, the molecules that were observed as mobile (D average

$> 500 \text{ nm}^2\text{s}^{-1}$), probed several rearranging regions and the values of the standard deviation of the diffusion coefficients are averaged dynamics.

ii) Heterogeneities are due to thin film dynamics. We assume that the T_g of our Pibma film of thickness $\sim 300 \text{ nm}$ is lower than that of bulk Pibma. The T_g shift are said to cause enhanced surface interface interactions at the polymer-air interface [15]. Enhanced interfacial interactions are a cause of reduced density ratio at the surface and as a result the probe molecule mobility is increased as temperature is increased. A reduction and variation in local density packing of the polymer chain segments may be assumed to directly influence the amount of free volume distribution within the film (Figure 30). A higher free volume distribution within the polymer film has a linear dependence on temperature from Doolittle's assumption on the free volume theory and thus facilitates the hopping of probe molecules within these vacant areas as the film relaxes via the β and α relaxation processes at the different temperature ranges.

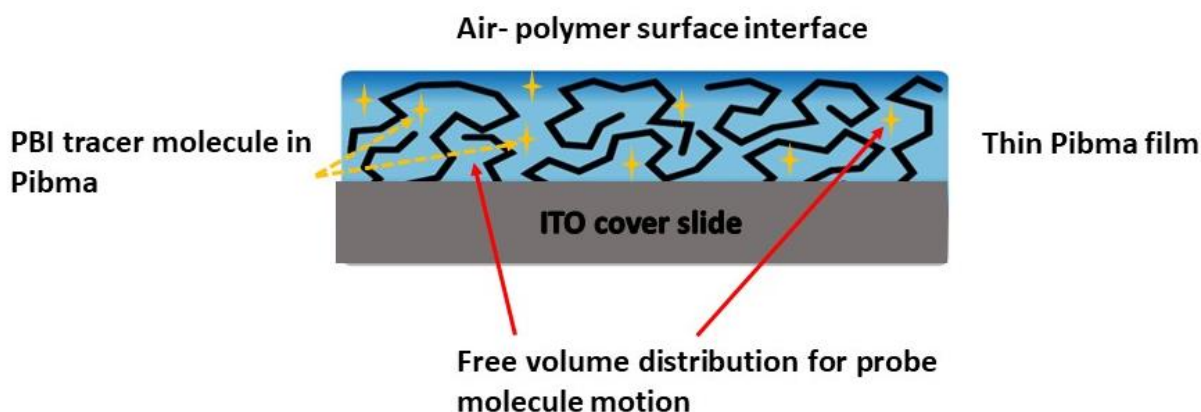


Figure 30. Enhanced surface interfacial interactions cause heterogeneities that contribute to T_g shifts in thin polymer samples as compared to their bulk counterparts [53], [54]. The reduced polymer chain density at the surface assists the diffusion motion of individual fluorescent tracers across the film, however the local density distribution of amorphous polymer chains is random thus the motion of the probe molecules is also expected to be inhomogeneous.

A final observation from PBI dye molecules embedded in Pibma thin films was the average fluorescence intensity decreased as the temperature was increased (Figure 31). Fluorescence intensity reduction may be a result of rotational diffusion of the PBI molecules in the polymer. However as has been stated in the design of the widefield optical set-up used for this work, the excitation laser light was circularly polarized to ensure uniform excitation, but the imaging section in this setup did not separate the fluorescence into vertical and horizontal polarization states which would have been sensitive to probe rotation, provided that the time scale falls with the temporal resolution of the setup.

Local density fluctuations in the polymer film influence the fluorescence emission of single molecules. The polymer film relaxes by local rearrangement of chain segments. The rearrangement of the chain segments influences changes in the local density or free volume redistribution within the polymer thereby affecting the emission of the dye molecules. One way of ascertaining that local density fluctuations in the polymer film affect the radiative lifetime of a probe molecule is by observing the trajectories of the fluctuating fluorescence lifetimes of the dye molecule as was done by [55]. A drawback from our set-up is inability to access the fluorescence lifetimes of the PBI molecules and hence study emission fluctuation patterns of dye molecule that are caused by the dynamics of the polymer segments.

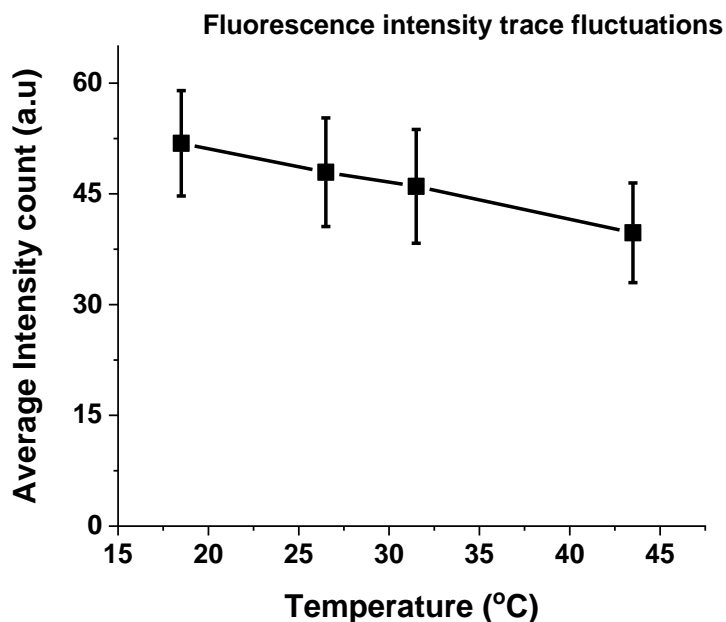


Figure 31. Decreasing average fluorescence intensity of PBI single molecules in Pibma as temperature was increased was observed.

The measurements of the photo physical parameters of PBI single molecules in two different polymer matrices was successful in illustrating the sensitivity of the widefield fluorescence microscopy set-up. From our results we were able to show both static and spatial heterogeneities of the two polymer films used in this work. However, improvements can be made to fully describe some of the observations noted that were not fully described. One notable improvement would be to increase the number of single molecules observed. The low number of molecules (typically 50) does not afford us the ability to provide conclusive description. However, we do see a qualitative trend for in all the parameters observed.

Chapter 5: Conclusions

The main objective of this research work was to apply single fluorescence microscopy in studying thin film polymer dynamics. Thin polymer film dynamics have shown puzzling and unique adjustable properties that are different to bulk polymer dynamics. These thin polymer film dynamics are known to influence the processing and application of polymers in various industries. Despite decades of research on polymers, the unique properties of thin polymer films have not been fully understood and thereby captivating the inquisitiveness of the scientific research field hence necessitating the need to further understand the connections between the macroscopic and microscopic properties of polymers.

Single molecule fluorescence microscopy was chosen as a technique to study polymer thin film dynamics since it is a powerful tool that enables the direct observation of single fluorescent molecules. Another advantage of the optical technique is the sensitivity of fluorescent probes to changes in their environment. To ensure the observation of single fluorescent molecules the concentration of the PBI dye solution was in the picomolar range thereby ensuring that dye molecules are sparsely spaced in the solution. The cover slide cleaning procedure also assisted in the observation of single molecules by eliminating any particulates that would have caused background fluorescence. Thin polymer film samples were prepared using the preparation protocol together with a spin coating procedure described in Chapter 3. The thickness measurements conducted using UV-Vis spectroscopy could estimate a thickness of ~ 900 nm for our thickest sample. The use of a tapping mode atomic force microscope can be used to verify the UV-Vis spectroscopy measurements as AFM tool is more equipped in determining thicknesses of samples.

The optical setup that was designed incorporated a wide field observation plane thus ensuring a large sample area was imaged. This was made possible by focusing a collimated excitation beam at the back-focal plane of a microscope objective. The polarization state of the excitation beam was successfully polarized to a circular state which then maximized the number of electric dipole moments of the single molecules to be uniformly excited. We were also able to achieve a localization precision of 20 nm. Microscope stage position stability measurements showed negligible drift thus the motion measured by the system as the diffusion of single molecules is indeed valid.

We were able to show the photophysical parameters of PBI dye molecules when exposed to different nano-environments thus illustrating the sensitivity of the optical setup built. From our results we were successful in studying the diffusion of single molecules in polymeric systems. Static and spatial heterogeneities in the polymers were observed and caused the fluorescence emission fluctuations of the PBI dye molecule as expected from literature even though we were unable to quantify radiative and triplet lifetimes of the PBI dye. Improvements can be made such that the extent of the heterogeneities of the polymer films can be described fully by increasing many sample molecules, some groups have conducted such measurements by studying and analyzing 160-205 molecules [4] and from our measurements we were studying and analyzing half the reported sample size. T_g shifts measurements reported from literature can also be investigated using this optical setup as a future work.

From this work we have shown proof of principle for sensitivity of single fluorescence microscopy applied to thin polymer film studies. These studies have also helped give us a basic understanding to the heterogeneities of thin polymer films and how these dynamics influence the diffusion of small probe molecules coupled to the relaxation processes of the polymer matrix at various temperature ranges. Our localization precision enabled the probing of averaged cooperatively rearranging regions which could have been obscured in bulk measurements and we were able to show that the Vogel-Fulcher relation for bulk polymers fails to account for these heterogeneities. The size of cooperatively rearranging regions can be probed by fluorescence imaging with one-nanometer accuracy (F.I.O.N.A) [56], however this technique is beyond the scope of this work.

BIBLIOGRAPHY

- [1] R. Geyer, J. R. Jambeck, and K. L. Law, "Production, use, and fate of all plastics ever made," *Sci. Adv.*, vol. 3, no. 7, Jul. 2017.
- [2] H. G. Schuster, "Complex Adaptive Systems," in *Collective Dynamics of Nonlinear and Disordered Systems*, Berlin/Heidelberg: Springer-Verlag, 2005, pp. 359–369.
- [3] W. E. Moerner and M. Orrit, "Illuminating single molecules in condensed matter.," *Science*, vol. 283, no. 5408, pp. 1670–6, Mar. 1999.
- [4] B. M. I. Flier *et al.*, "Heterogeneous diffusion in thin polymer films as observed by high-temperature single-molecule fluorescence microscopy.," *J. Am. Chem. Soc.*, vol. 134, no. 1, pp. 480–8, Jan. 2012.
- [5] R. A. L. Vallée *et al.*, "Fluorescence lifetime fluctuations of single molecules probe the local environment of oligomers around the glass transition temperature," *J. Chem. Phys.*, vol. 126, no. 18, p. 184902, May 2007.
- [6] W. Callister and D. Rethwisch, "Materials science and engineering: an introduction," in *Materials Science and Engineering*, William D., vol. 94, A. M. Joseph Hayton, Ken Santor, Ed. 605 Third Avenue, New York, NY 10158-0012, (212) 850-6011: John Wiley & Sons, Inc., 2007, p. 492.
- [7] Michalovic Mark, "sty03." [Online]. Available: <http://www.pslc.ws/macrog/styrene.htm>.
- [8] FimmTech Inc, "amorphous&semi-crystalline," *Fimmtech, Resources for scientific moulding and processing.*, 2018. [Online]. Available: <http://fimmtech.com/knowledgebase/polymers-and-plastics/#thermal-transitions>. [Accessed: 02-May-2018].
- [9] B. M. I. Flier *et al.*, "Single molecule fluorescence microscopy investigations on heterogeneity of translational diffusion in thin polymer films," *Phys. Chem. Chem. Phys. Phys. Chem. Chem. Phys.*, vol. 13, no. 13, pp. 1770–1775, 2011.
- [10] FimmTech Inc, "Tg," *Fimmtech, Resources for scientific moulding and processing.*, 2018. [Online]. Available: <http://fimmtech.com/knowledgebase/polymers-and-plastics/>. [Accessed: 02-May-2018].
- [11] P. H. Li and P. K. Chu, "Thin film deposition technologies and processing of biomaterials," *Thin Film Coatings Biomater. Biomed. Appl.*, pp. 3–28, Jan. 2016.
- [12] N. S. Murthy, V. B. Damodaran, S. H. Lee, A. S. Hwang, and H.-J. Sung, "Characterization of thin films for biomedical applications," *Thin Film Coatings Biomater. Biomed. Appl.*, pp. 81–115, Jan. 2016.
- [13] M. Mozafari, A. Ramedani, Y. N. Zhang, and D. K. Mills, "Thin films for tissue engineering applications," *Thin Film Coatings Biomater. Biomed. Appl.*, pp. 167–195, Jan. 2016.
- [14] D. Wöll, E. Braeken, A. Deres, F. C. De Schryver, H. Uji-i, and J. Hofkens, "Polymers and single molecule fluorescence spectroscopy, what can we learn?," *Chem. Soc. Rev.*, vol. 38, no. 2, pp. 313–328, 2009.

- [15] M. D. Ediger and J. A. Forrest, "Dynamics near free surfaces and the glass transition in thin polymer films: A view to the future," *Macromolecules*, vol. 47, no. 2, pp. 471–478, Jan. 2014.
- [16] T. S. Chow, *Glassy—State Relaxation*. 2000.
- [17] M. L. Williams, R. F. Landel, and J. D. Ferry, "The Temperature Dependence of Relaxation Mechanisms in Amorphous Polymers and Other Glass-forming Liquids," *J. Am. Chem. Soc.*, vol. 77, no. 14, pp. 3701–3707, Jul. 1955.
- [18] C. Donati, S. C. Glotzer, P. H. Poole, W. Kob, and S. J. Plimpton, "Spatial correlations of mobility and immobility in a glass-forming Lennard-Jones liquid," *Phys. Rev. E - Stat. Physics, Plasmas, Fluids, Relat. Interdiscip. Top.*, vol. 60, no. 3107, 1999.
- [19] J. Heijboer, J. M. A. Baas, B. van de Graaf, and M. A. Hoefnagel, "A molecular mechanics study on rotational motions of side groups in poly(methyl methacrylate)," *Polymer (Guildf.)*, vol. 28, no. 3, pp. 509–513, Mar. 1987.
- [20] P. RA, "Polymer physics. Edited by Michael Rubinstein and Ralph H Colby Oxford University Press, Oxford, 2003. ISBN 019852059X. pp 440," *Polym. Int.*, vol. 53, no. 9, pp. 1394–1395, Jul. 2004.
- [21] A. K. Doolittle, "Studies in Newtonian Flow. II. The Dependence of the Viscosity of Liquids on Free-Space," *J. Appl. Phys.*, vol. 22, no. 12, pp. 1471–1475, Dec. 1951.
- [22] L. H. Sperling, *Introduction to Physical Polymer Science: Fourth Edition*. Hoboken, NJ, USA: John Wiley & Sons, Inc., 2005.
- [23] M. L. Ferrer, C. Lawrence, B. G. Demirjian, D. Kivelson, C. Alba-Simionesco, and G. Tarjus, "Supercooled liquids and the glass transition: Temperature as the control variable," *J. Chem. Phys.*, vol. 109, no. 18, pp. 8010–8015, Nov. 1998.
- [24] J. H. Gibbs and E. A. DiMarzio, "Nature of the Glass Transition and the Glassy State," *J. Chem. Phys.*, vol. 28, no. 3, pp. 373–383, Mar. 1958.
- [25] N. Giovambattista, S. V. Buldyrev, F. W. Starr, and H. E. Stanley, "Connection between Adam-Gibbs Theory and Spatially Heterogeneous Dynamics," *Phys. Rev. Lett.*, vol. 90, no. 8, p. 085506, Feb. 2003.
- [26] Q. Zheng and J. C. Mauro, "Viscosity of glass-forming systems," *J. Am. Ceram. Soc.*, vol. 100, no. 1, pp. 6–25, 2017.
- [27] F. W. D. Rost, *Fluorescence microscopy*. New York: Cambridge University Press, 1992.
- [28] O. van den Berg, W. G. F. Sengers, W. F. Jager, S. J. Picken, and M. Wübbenhorst, "Dielectric and Fluorescent Probes To Investigate Glass Transition, Melt, and Crystallization in Polyolefins," *Macromolecules*, vol. 37, no. 7, pp. 2460–2470, Apr. 2004.
- [29] G. Modesti, B. Zimmermann, M. Börsch, A. Herrmann, and K. Saalwächter, "Diffusion in Model Networks as Studied by NMR and Fluorescence Correlation Spectroscopy," *Macromolecules*, vol. 42, no. 13, pp. 4681–4689, Jul. 2009.
- [30] J. K. Trautman and J. J. Macklin, "Time-resolved spectroscopy of single molecules using near-field and far-field optics," *Chem. Phys.*, vol. 205, no. 1–2, pp. 221–229, 1996.

- [31] G. Zhang, L. Xiao, F. Zhang, X. Wang, and S. Jia, "Single molecules reorientation reveals the dynamics of polymer glasses surface," *Phys. Chem. Chem. Phys.*, vol. 12, no. 10, pp. 2308–2312, 2010.
- [32] A. Schob, F. Cichos, J. Schuster, and C. Von Borczyskowski, "Reorientation and translation of individual dye molecules in a polymer matrix," *Eur. Polym. J.*, vol. 40, no. 5, pp. 1019–1026, 2004.
- [33] M. D. Tyona, "A theoretical study on spin coating technique," *Adv. Mater. Res.*, 2013.
- [34] N. Tomczak *et al.*, "Probing polymers with single fluorescent molecules," *Eur. Polym. J.*, vol. 40, no. 5, pp. 1001–1011, May 2004.
- [35] S. B. Petersen, T. Viruthachalam, I. Coutinho, G. P. Gajula, and M. T. Neves-Petersen, "Image processing for drift compensation in fluorescence microscopy," 2013, vol. 8587, p. 85871H.
- [36] R. A. L. Vallé, N. Tomczak, G. J. Vancso, L. Kuipers, and N. F. Van Hulst, "Fluorescence lifetime fluctuations of single molecules probe local density fluctuations in disordered media: A bulk approach," *J. Chem. Phys.*, vol. 122, no. 11, 2005.
- [37] J. S. Vrentas and C. M. Vrentas, "Evaluation of the free-volume theory of diffusion," *J. Polym. Sci. Part B Polym. Phys.*, vol. 41, no. 5, pp. 501–507, Mar. 2003.
- [38] Y. Lill and B. Hecht, "Single dye molecules in an oxygen-depleted environment as photostable organic triggered single-photon sources," *Appl. Phys. Lett.*, vol. 84, no. 10, pp. 1665–1667, Mar. 2004.
- [39] M. F. García-Parajó, J. A. Veerman, R. Bouwhuis, R. Vallée, and N. F. Van Hulst, "Optical probing of single fluorescent molecules and proteins," *ChemPhysChem*, vol. 2, no. 6. Wiley-VCH Verlag, pp. 347–360, 18-Jun-2001.
- [40] M. Talhavini, W. Corradini, and T. D. Z. Atvars, "The role of the triplet state on the photobleaching processes of xanthene dyes in a poly(vinyl alcohol) matrix," *J. Photochem. Photobiol. A Chem.*, vol. 139, no. 2–3, pp. 187–197, Mar. 2001.
- [41] R. H. D. Miora, "Point Spread Function Engineering for Fluorescence Microscopy," 2018.
- [42] J. B. Pawley, *Handbook of biological confocal microscopy: Third edition*. Boston, MA: Springer US, 2006.
- [43] C. Lu, M. Fujitsuka, A. Sugimoto, and T. Majima, "Unprecedented Intramolecular Electron Transfer from Excited Perylenediimide Radical Anion," *J. Phys. Chem. C*, vol. 120, no. 23, pp. 12734–12741, Jun. 2016.
- [44] E. E. Neuteboom, "Photoinduced processes of functionalized perylene bisimides."
- [45] K. A. Kneas, J. N. Demas, B. Nguyen, A. Lockhart, W. Xu, and B. A. DeGraff, "Method for measuring oxygen diffusion coefficients of polymer films by luminescence quenching," *Anal. Chem.*, vol. 74, no. 5, pp. 1111–8, Mar. 2002.
- [46] A. Thran, C. Kroll, and F. Faupel, "Correlation between fractional free volume and diffusivity of gas molecules in glassy polymers," *J. Polym. Sci. Part B Polym. Phys.*, vol. 37, no. 23, pp. 3344–3358, Dec. 1999.

- [47] I. F. Sbalzarini and P. Koumoutsakos, "Feature point tracking and trajectory analysis for video imaging in cell biology," *J. Struct. Biol.*, vol. 151, no. 2, pp. 182–195, Aug. 2005.
- [48] A. Einstein, "On the Motion of Small Particles Suspended in a Stationary Liquid," *Ann. Phys.*, vol. 322, pp. 549–560, 1905.
- [49] J. M. Katzenstein, D. W. Janes, H. E. Hocker, J. K. Chandler, and C. J. Ellison, "Nanoconfined Self-Diffusion of Poly(isobutyl methacrylate) in Films with a Thickness-Independent Glass Transition," *Macromolecules*, vol. 45, no. 3, pp. 1544–1552, Feb. 2012.
- [50] R. A. L. Vallée, N. Tomczak, L. Kuipers, G. J. Vancso, and N. F. van Hulst, "Single Molecule Lifetime Fluctuations Reveal Segmental Dynamics in Polymers," *Phys. Rev. Lett.*, vol. 91, no. 3, p. 038301, Jul. 2003.
- [51] S. A. Reinsberg, X. H. Qiu, M. Wilhelm, H. W. Spiess, and M. D. Ediger, "Length scale of dynamic heterogeneity in supercooled glycerol near T_g ," *J. Chem. Phys.*, vol. 114, no. 17, pp. 7299–7302, 2001.
- [52] C. J. Ellison and J. M. Torkelson, "The distribution of glass-transition temperatures in nanoscopically confined glass formers," *Nat. Mater.*, vol. 2, no. 10, pp. 695–700, Oct. 2003.
- [53] B. Zuo, Y. Liu, Y. Liang, D. Kawaguchi, K. Tanaka, and X. Wang, "Glass Transition Behavior in Thin Polymer Films Covered with a Surface Crystalline Layer," *Macromolecules*, vol. 50, no. 5, pp. 2061–2068, 2017.
- [54] M. Crawford, "Committed to quality.," *Nursing (Lond)*, vol. 4, no. 9, pp. 30–4, 94AD.
- [55] R. A. L. Vallée, M. Van Der Auweraer, F. C. De Schryver, D. Beljonne, and M. Orrit, "A microscopic model for the fluctuations of local field and spontaneous emission of single molecules in disordered media," *ChemPhysChem*, vol. 6, no. 1, pp. 81–91, 2005.
- [56] H. Kim and P. R. Selvin, "Fluorescence Imaging with One Nanometer Accuracy," *Encycl. Biophys.*, no. 91, pp. 1–7, Sep. 2018.
- [57] "Biotin and Hapten Derivatives Molecular Probes™ Handbook A Guide to Fluorescent Probes and Labeling Technologies 11th Edition (2010) Fluorophores and Their Amine-Reactive Derivatives The Molecular Probes® Handbook A GUIDE TO FLUORESCENT PROBES AND LABELI."